U.S. Department of the Interior
U.S. Geological Survey

Geochemistry and Hydrogeologic Framework of the Saline-Freshwater Interface and the Calculation of Net Recharge in the Dorado Area, North-Central Puerto Rico

Prepared in cooperation with the

PUERTO RICO AQUEDUCT AND SEWER AUTHORITY

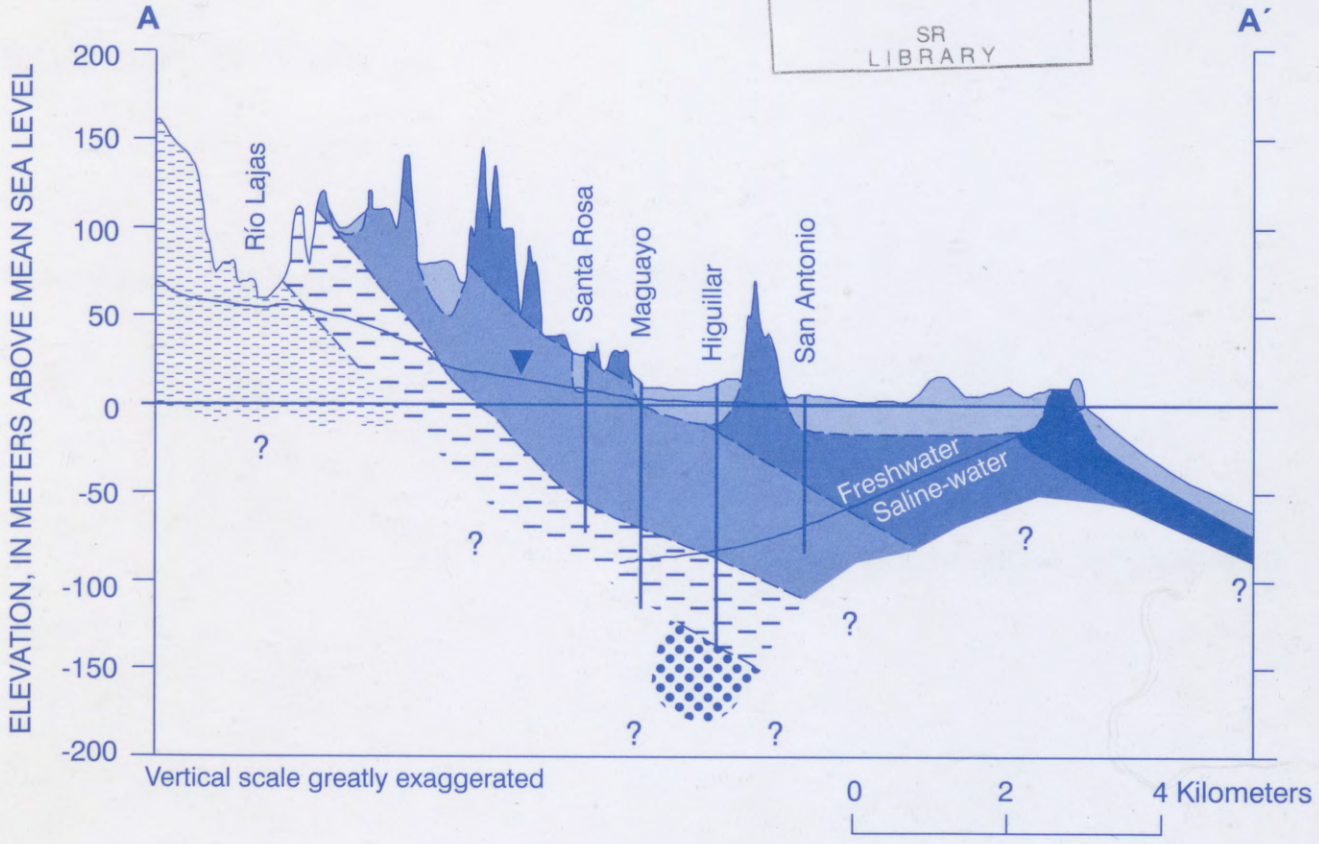

WATER-RESOURCES INVESTIGATIONS REPORT 98-4030

USGS
science for a changing world

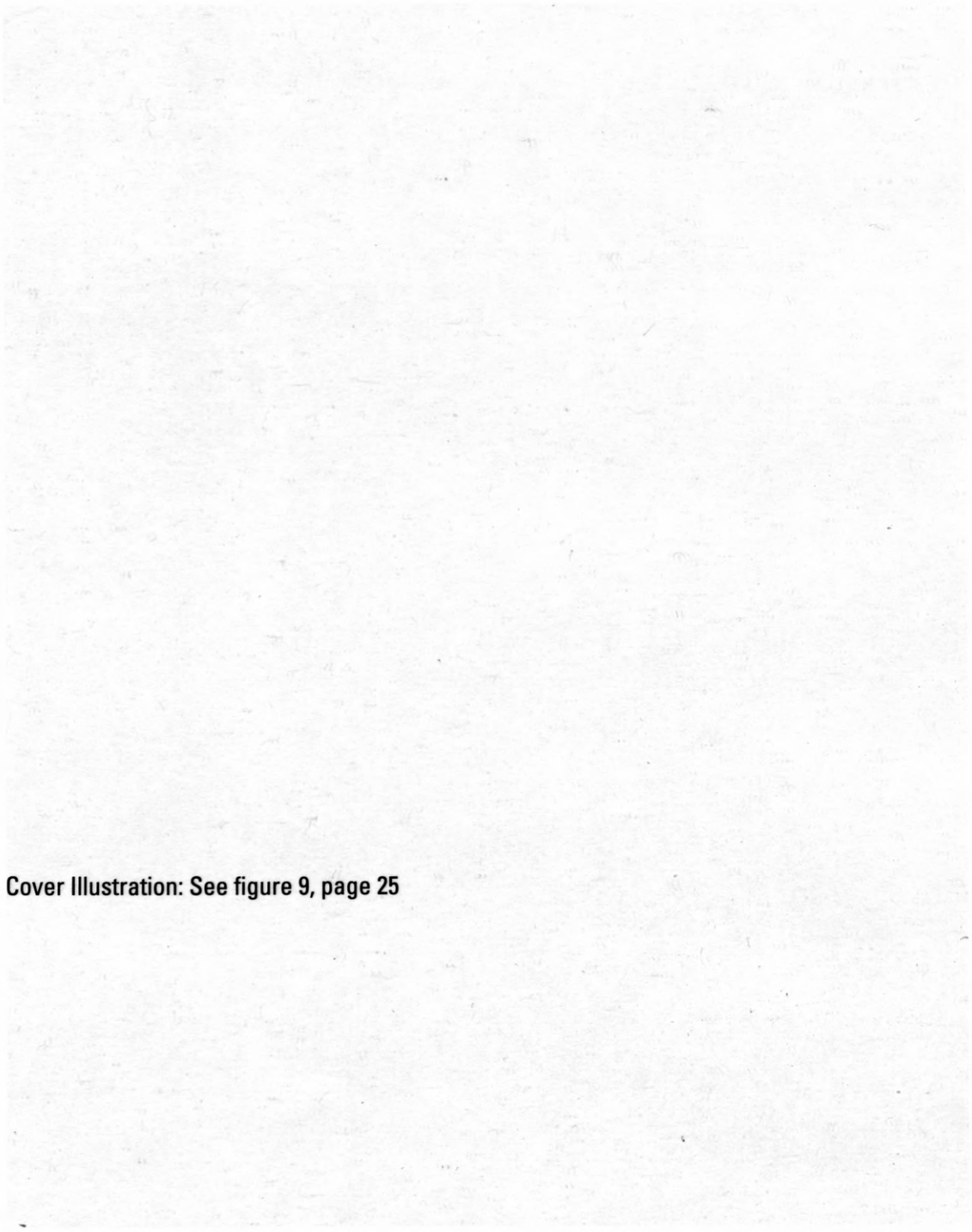

Cover Illustration: See figure 9, page 25

U.S. Department of the Interior
U.S. Geological Survey

Geochemistry and Hydrogeologic Framework of the Saline-Freshwater Interface and the Calculation of Net Recharge in the Dorado Area, North-Central Puerto Rico

By Joseph W. Troester

Water-Resources Investigations Report 98–4030

Prepared in cooperation with the

PUERTO RICO AQUEDUCT AND SEWER AUTHORITY

San Juan, Puerto Rico: 1999

U.S. DEPARTMENT OF THE INTERIOR
BRUCE BABBITT, Secretary

U.S. GEOLOGICAL SURVEY
Charles G. Groat, Director

The use of firm, trade, and brand names in this report is for identification purposes only and does not constitute endorsement by the U.S. Government.

For additional information write to:

District Chief
U.S. Geological Survey
GSA Center, Suite 400-15
651 Federal Drive
Guaynabo, Puerto Rico 00965-5703

Copies of this report can be purchased from:

U.S. Geological Survey
Branch of Information Services
Box 25286
Denver, CO 80225-0286

CONTENTS

FIGURES

TABLES

CONVERSION FACTORS AND ABBREVIATED UNITS

Multiply	By	To obtain
kilometer (km)	0.62137	mile
meter (m)	3.2808	feet
centimeter (cm)	0.3937	inch
millimeter (mm)	0.03937	inch
micrometer (µm)	0.00003937	inch
square kilometer (km^2)	0.3861	square mile
cubic meter per second (m^3/s)	35.31	cubic foot per second
cubic meter per second (m^3/s)	15,850.	gallon per minute
meter squared per day (m^2/d)	0.05592	gallon per minute per foot

Temperature: In this report temperatures are given in degrees Celsius (°C). Temperatures may be converted to degrees Fahrenheit (°F) as follows:

$°F = (9/5 \times °C) + 32$

Abbreviated water-quality, concentration, and geophysical units used in this report:

micrograms per liter (µg/L)
milligrams per liter (mg/L)
microsiemens per centimeter at 25 °C (µS/cm)
millisiemens per meter (mS/m)

Microsiemens per centimeter can be converted to millisiemens per meter as follows:

10 µS/cm = mS/m

Geochemistry and Hydrologic Framework of the Saline-Freshwater Interface and the Calculation of Net Recharge in the Dorado Area, North-Central Puerto Rico

By **Joseph W. Troester**

Abstract

The upper aquifer near Dorado, Puerto Rico, is a major source of water for both public and private supply. The aquifer is composed of portions of the Aguada Limestone, Aymamón Limestone, and adjacent permeable portions of unconsolidated deposits. As water moves through the aquifer it changes from a calcium-bicarbonate type water in the upgradient portions of the aquifer to a sodium-chloride type water in the downgradient portions of the aquifer near the coast. Pumping from the aquifer for industrial use and public supply has lowered the water table to near sea level in some areas, causing saline intrusion to be a concern. The saline-freshwater interface was located by drilling and borehole geophysics. Drilling and borehole geophysics helped locate the lower limit of the aquifer. The saline-freshwater interface is narrow close to the coast and thickens with distance from the coast. Ground-water hydrographs in the study area were simulated with a deterministic model that allows net recharge to be calculated from precipitation data and ground-water level data. Calculated net recharge rates ranged from 160 millimeters per year in 1995 at the Santa Rosa well site to 260 millimeters per year in 1996 at the Maguayo well site.

INTRODUCTION

The carbonate aquifer, in the Dorado area, just west of the San Juan area in north-central Puerto Rico, supplies water for domestic, commercial, and industrial uses. The development of ground-water supplies in this and other areas along the north-central coast of Puerto Rico is limited by saline-water intrusion. In 1991, the U.S. Geological Survey (USGS), in cooperation with the Puerto Rico Aqueduct and Sewer Authority (PRASA) began an investigation to study the hydrogeology and geochemistry of the aquifer in order to better understand the controls on saline intrusion in the area.

Purpose and Scope

This report describes the geochemistry and hydrogeologic framework of the saline-freshwater interface in the aquifer near Dorado, Puerto Rico, and the calculation of net recharge to the aquifer. The study area covers most of the USGS Vega Alta and Bayamón 7.5-minute topographic quadrangle maps (fig. 1). In this report, the study area is named after the municipality of Dorado, even though the Vega Alta and Bayamón quadrangles include all or parts of the municipalities of Bayamón, Cataño, Dorado, Guaynabo, Toa Alta, Toa Baja, Vega Alta, and Vega Baja.

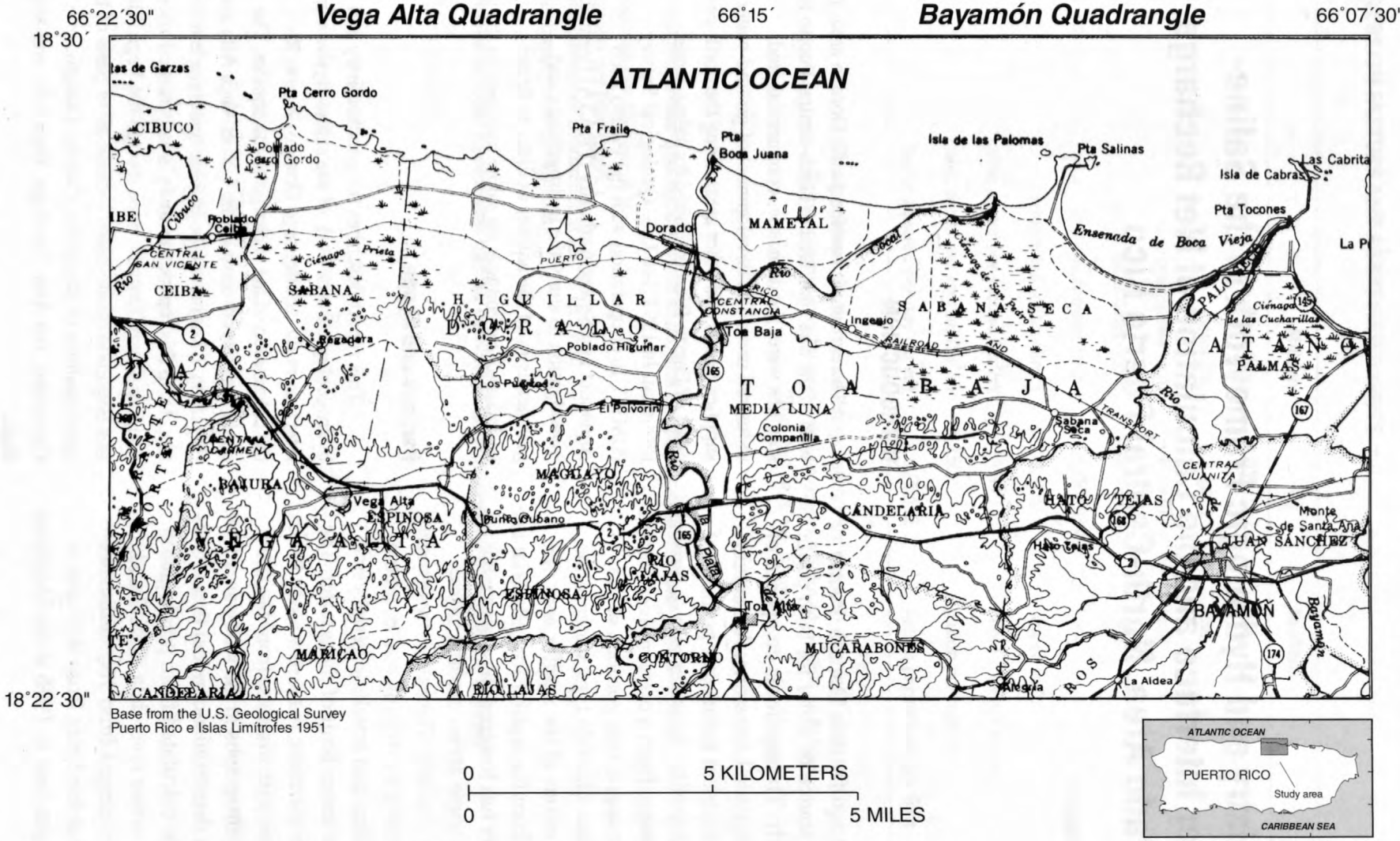

Figure 1. The topography of the Dorado area, north-central Puerto Rico.

The scope of the investigation included the collection and evaluation of ground-water quality and other ground-water data. Water-quality samples were collected from nine existing wells in March and April 1992. Thirteen observation wells were drilled in the study area at five sites to determine and monitor the location of the saline-freshwater interface and to provide sites for measuring changes in the water-table elevation in response to local precipitation. The observation wells were constructed between October 1993 and April 1995. Borehole geophysical tools were used to determine the location of the saline-freshwater interface in these observation wells and other wells in May 1995. Continuous water-level data from several of these observation wells and other wells were collected with ADR's (analog digital recorders) from after their completion until December 1996, a period of about 1 to 3 years. Ground-water level data from the observation wells were analyzed and compared with precipitation data to estimate net recharge at selected sites in the study area. The observation wells have been and are expected to continue to be useful for monitoring the upper aquifer for movement of the saline-freshwater interface.

Acknowledgments

The author would like to acknowledge the assistance of Ronald T. Richards, who collected the borehole geophysical data, and Vanessa I. Monell-González, who as a graduate student in geology at Queens College in New York collected the geochemical data.

DESCRIPTION OF THE DORADO AREA

Geology

Puerto Rico has a central mountainous area composed of Late Jurassic to Eocene volcanic and sedimentary rocks and Late Cretaceous granodiorite plutons. A section of nearly horizontal middle Oligocene to Pliocene limestones and terrigenous sediments unconformably overlies the older rocks along the north side of the island and comprises the northern karst belt, a 10- to 20-km-wide strip of karst topography that extends along the northwest and north-central coast of Puerto Rico (Briggs and Akers, 1965). These rocks consist of a sequence of limestones and terrigenous sediments of Oligocene to Pliocene age that strike east-west and normally dip 2 to 5 degrees toward the north. Several geologists have described these rocks and divided them into formations (Berkey, 1915, 1919; Semmes, 1919; Hubbard, 1920, 1923; Zapp and others, 1948; Monroe, 1973b, 1975, 1980a; Meyerhoff, 1975; Moussa and Seiglie, 1975; Frost and others, 1983; Seiglie and Moussa, 1984; Moussa and others, 1987; Monell-González and González, 1993; Monell-González, 1994). There is still some debate over the names, but most researchers now divide the sequence into seven formations. In order of decreasing age, the formations are the San Sebastián Formation, Lares Limestone, Mucarabones Sand, Cibao Formation, Aguada Limestone (which is referred to as the Los Puertos Limestone by some authors, including Meyerhoff (1975) and Moussa and Seiglie (1975)), Aymamón Limestone, and Camuy Formation (which is referred to as the Quebradillas Formation by some authors, including Moussa and others (1987)). Monroe (1963, 1973a, 1973b, 1975, 1980a) described all seven formations in detail. Monroe (1963, 1973a) mapped the surface geology of the area near Dorado at a scale of 1:20,000. Veve and Taggart (1996) recently published a generalized geologic map of the Dorado area, which has been adapted for figure 2. Figure 3 is a schematic geologic column that shows the approximate variation in thickness of the geologic units across the Vega Alta and Bayamón quadrangles.

The oldest unit of this sequence in the study area is the Oligocene (to possibly Miocene) age Mucarabones Sand (Monroe, 1980a). Originally these deposits were mapped by Monroe and Pease (1962) and Monroe (1963) as the San Sebastián Formation, but later were assigned the name Mucarabones Sand by Nelson (1966). The Mucarabones Sand consists primarily of cross-bedded grayish-orange and yellow fine- to medium-grained sand. The maximum thickness of the Mucarabones Sand is about 120 m in the center of the Bayamón quadrangle. The unit thins to about 90 m at the eastern edge of the Bayamón quadrangle and to about 70 m in the southeastern corner of the Vega Alta quadrangle (Monroe, 1963, 1973a, 1980a).

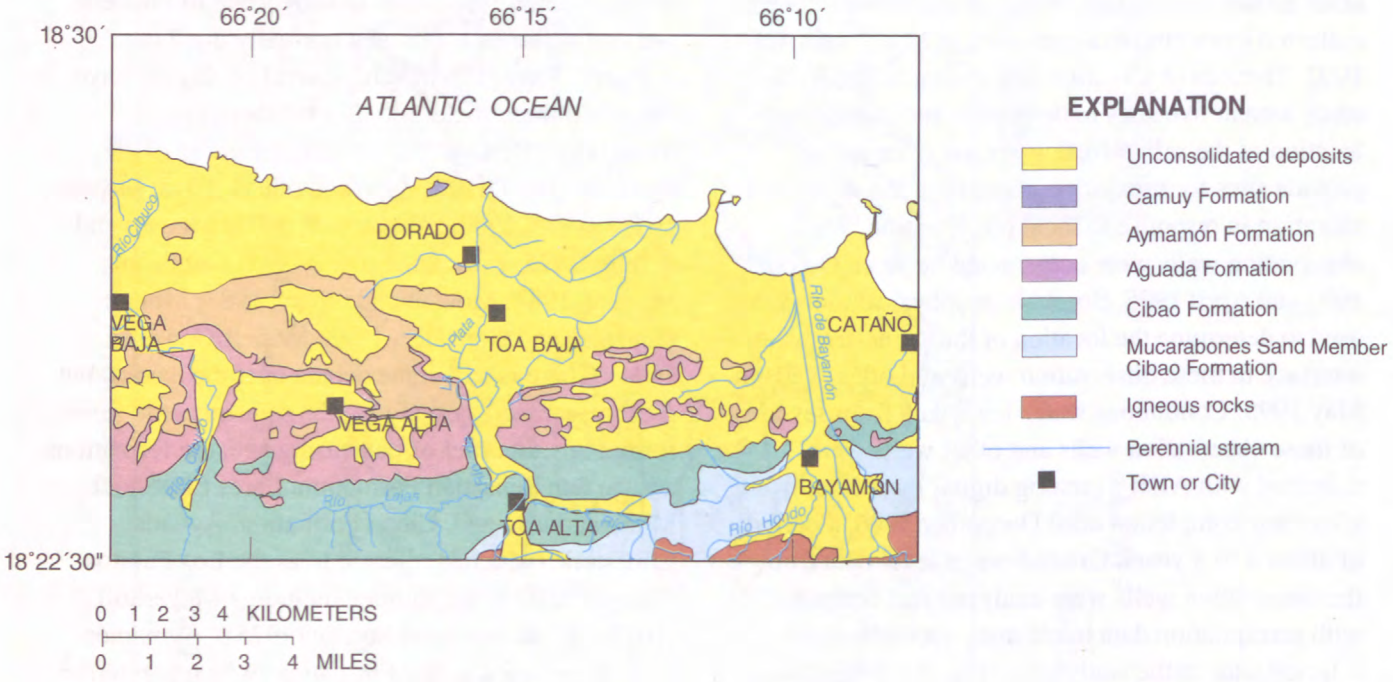

Figure 2. Generalized surface geology of the Dorado area, north-central Puerto Rico (Adapted from Monroe 1963, 1973a; Veve and Taggart, 1996).

The early Miocene age Cibao Formation overlies the Lares Limestone and grades laterally into the Mucarabones Sand (Seiglie and Moussa, 1984). Hubbard (1920, 1923) was the first to name and describe the Cibao Formation. The Cibao Formation is a heterogeneous unit consisting of "intergradational and interlensing beds of calcareous clay, limestone, sandy clay, sand, sandstone, and gravel" (Monroe, 1980a). Consequently, the Cibao Formation has been divided into several members; however, only four are present in the study area: the Río Indio Limestone Member, the Quebrada Arenas Limestone Member, the Miranda Sand Member, and the informally named upper member. The total thickness of the Cibao Formation where it is exposed at the surface ranges from about 200 m at the western edge of the Vega Alta quadrangle to about 50 m at the eastern edge of the Bayamón quadrangle (Monroe, 1963, 1973a). More recently, the USGS drilled a number of test holes to describe the aquifers in the north coast limestones. The NC–8 test hole is approximately in the center of the Vega Alta quadrangle. The lithology of this test hole was described by Scharlach (1990) and Rodríguez-Martínez and Scharlach (1994). They described the rock cores from NC–8 and reported the thickness of the Cibao Formation in the subsurface to be about 160 m.

The Río Indio Limestone Member of the Cibao Formation consists of dark yellowish orange, thick-bedded limestone. The unit ranges in thickness from about 100 m in the western part of the Vega Alta quadrangle to 0 m as the unit grades into the Mucarabones Sand near the center of the Bayamón quadrangle (Monroe, 1963, 1973a, 1980a).

The Quebrada Arenas Limestone Member of the Cibao Formation consists of hard very pale orange fossiliferous crystalline limestone and hard very pale orange to grayish-orange calcarenite. The unit ranges in thickness from about 60 m in the western part of the Vega Alta quadrangle to 0 m as the unit grades into the Mucarabones Sand towards the eastern part of the Bayamón quadrangle (Monroe, 1963, 1973a, 1980a).

The Miranda Sand Member of the Cibao Formation is a discontinuous unit found in channels eroded in the top of the Quebrada Arenas Limestone Member. This mottled grayish red and yellowish gray unit consists of a maximum of 15 m of coarse sand in a silty and clayey non-calcareous matrix (Monroe, 1963, 1973a, 1980a).

According to Monroe (1963, 1973a), the upper 50 m of the Cibao Formation in the study area are the informally named upper member of the Cibao Formation. Scharlach (1990) and Rodríguez-Martínez and Scharlach (1994) reported a thickness of about 97 m for the upper unit of the Cibao Formation in the subsurface at the NC–8 test hole. Monroe (1963) described the upper member of the Cibao Formation as "white to yellow chalk and calcareous claystone, generally massive, but locally in layers 5 to 10 mm thick. Locally it also contains beds of semi-indurated, compact, clayey, generally rubbly limestone."

The middle Miocene age (Seiglie and Moussa, 1984) Aguada Limestone (or Los Puertos Limestone) rests conformably on the Cibao Formation and the contact between the two is gradational. The Los Puertos Limestone was first named and described by Hubbard (1920, 1923). Zapp and others (1948) discarded this name and used the name Aguada Limestone for some transitional beds between the Cibao Formation and their Aymamón Limestone. Unfortunately, after the name became entrenched in the literature, Monroe (1968) found that the type section of the Aguada Limestone was in the Cibao Formation and that most of the rocks mapped as Aguada Limestone were equivalent to the Los

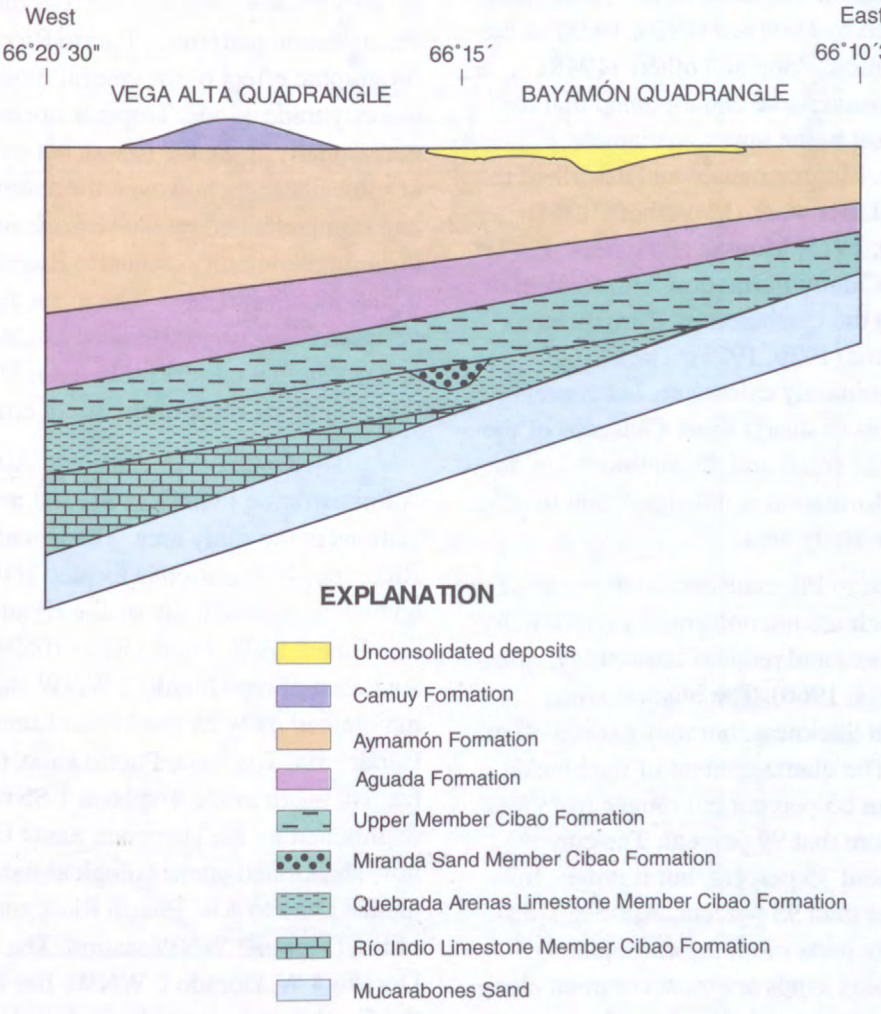

Figure 3. Schematic geologic column showing the approximate variation in thickness of the geologic units in the Dorado area, north-central Puerto Rico.

Puertos Limestone of Hubbard. The rock is a fine- to medium-grained calcarenite, with some quartz sand. The uppermost few meters of the Aguada Limestone are usually a thin-bedded cross-laminated limestone (Seiglie and Moussa, 1984). The unit is 90 m thick on the western border of the Vega Alta quadrangle, but it thins to 35 m in the eastern part of the Bayamón quadrangle (Monroe, 1963, 1973a).

The middle Miocene age Aymamón Limestone conformably overlies the Aguada Limestone (Seiglie and Moussa, 1984). Zapp and others (1948) named the Aymamón Limestone, but the base and top of the Aymamón Limestone were more carefully defined in Monroe (1963, 1968). About 200 m of this thick-bedded to massive, pure limestone is exposed in the Dorado area (Monroe, 1963, 1973a).

The youngest rock unit in the northern karst belt is the Camuy Formation. These rocks were originally named and described by Hubbard (1920, 1923) as the Quebradillas Formation. Zapp and others (1948) discarded this formation name and assumed that the rocks were equivalent to the upper Aymamón Limestone. In 1963, Monroe named and described the Camuy Formation. Later work (Meyerhoff, 1975; Moussa and Seiglie, 1975; Moussa and others, 1987) has shown that the Camuy Formation is equivalent or nearly equivalent to the Quebradillas Formation described by Hubbard (1920, 1923). The Camuy Formation is predominantly calcareous but contains considerable amounts of quartz sand. Outcrops of the Camuy Formation are small and discontinuous in the study area and this formation is not significant to the hydrogeology of the study area.

The Oligocene to Pliocene carbonate rocks of the northern karst belt are unconformably overlain by a deposit of quartz sand and reddish-brown clay, called blanket sands (Briggs, 1966). The blanket sands average 4 to 10 m in thickness, but may exceed 30 m in some locations. The quartz content of the blanket sands averages about 65 percent but ranges from less than 5 percent to more that 99 percent. The clay content averages about 35 percent, but it ranges from less than 1 to greater than 95 percent. Although the blanket sands overlie parts of all the carbonate formations, the blanket sands are most common along the northern edge of the karst belt, where they overlie the Aguada Limestone and the Aymamón Limestone in intrakarst plains which are as much as 8 km long.

In addition to the blanket sands, a variety of other unconsolidated and semi-consolidated Quaternary deposits can be found in the study area adjacent to the major rivers and near the coast. These deposits include Pleistocene river-terrace deposits, deltaic and mud-flat deposits, beach deposits, and eolianites, as well as Holocene landslide debris, alluvium, swamp deposits, beach deposits, and reef deposits. All of these Quaternary deposits were mapped and described by Monroe (1963, 1973a). The Quaternary deposits with sufficient areal extent are shown in figure 2.

Climate

The mean annual temperature of Puerto Rico is about 25°C (Calvesbert, 1970). Nearly constant easterly trade winds occur across the island. Precipitation patterns in Puerto Rico are a result of the orographic effect of the central mountains on these easterly trade winds. Tropical storms and hurricanes occasionally strike the island, but more often they pass at some distance; however, the anomalously high wind and rain generated by the passage of these storms through the vicinity of Puerto Rico can affect the island for several days. The mean annual precipitation varies across Puerto Rico and ranges from more than 4,000 mm in a rain forest in the northeast to less than 900 mm along most of the south coast.

The National Oceanic and Atmospheric Administration maintains several meteorological stations in the study area. The Dorado 2 WNW, Puerto Rico, (663409) station is located at the Dorado Airport and is maintained daily by the Hyatt Beach Hotel. The Toa Baja 1 SSW, Puerto Rico, (669421) station lies southeast of the Dorado 2 WNW station and is maintained daily by the Media Luna Dairy. The Candelaria, Toa Baja, Puerto Rico, (661536) station is located south of the Toa Baja 1 SSW station and is maintained by the Hacienda Santa Elena. An older, now abandoned, meteorological station in the area was named Dorado 4 W, Puerto Rico, and was located west of the Dorado 2 WNW station. The locations of the Dorado 4 W, Dorado 2 WNW, Toa Baja 1 SSW, and the Candelaria meteorological stations are shown in figure 4 with the symbols M1, M2, M3, and M4, respectively.

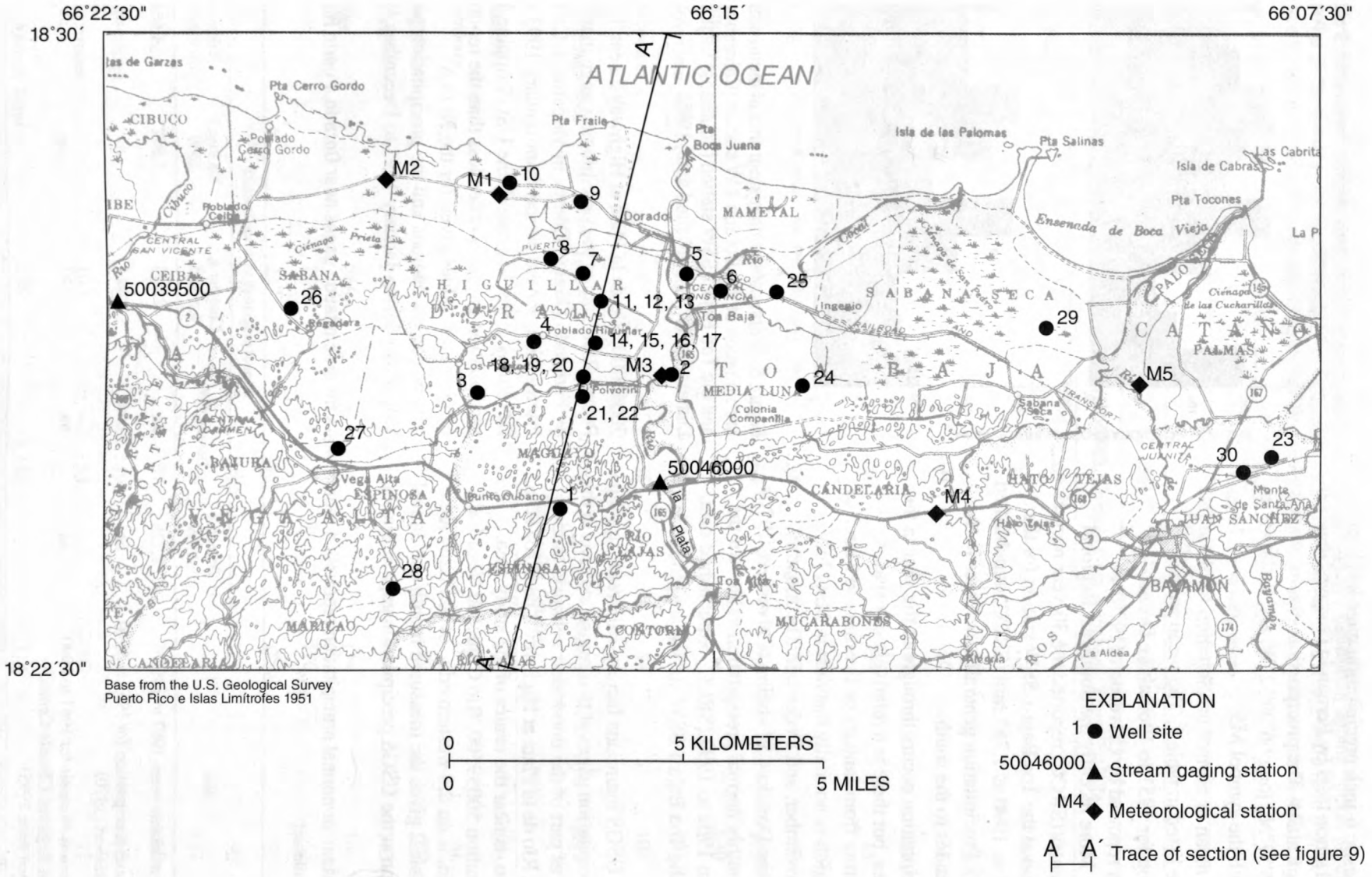

Figure 4. Location of selected wells, meteorological stations, and surface-water stations in the Dorado area, north-central Puerto Rico.

A plastic 6-inch precipitation gage has been maintained since 1993 by Fernando Gómez-Gómez in Valparaíso, Cataño. The precipitation gage is located at lat 18°25'57"N., long 66°09'52"W. and is shown in figure 4 with the symbol M5.

The mean or normal precipitation for these five stations are listed in table 1. The mean annual precipitation for 1951 to 1960 at the Dorado 4 W station was reported by Calvesbert (1970) as 1,655 mm. More recently the Southeast Regional Climate Center (SRCC) reported the 30-year normal precipitation at the Toa Baja 1 SSW station for the years 1961 to 1990 as 1,767 mm (SRCC, unpublished data, 1995). Precipitation generally increases in the higher altitudes to the south.

Precipitation occurs throughout the year in the Dorado area, but there is a relatively dry season, usually lasting from January or February to March or April. Rainfall is normally heaviest in May, July, August, November, and December. The monthly means for the Dorado 4 W station (Calvesbert, 1970) and the monthly normal precipitation values for the period from 1961 to 1990 (SRCC, unpublished data, 1995) for the Toa Baja 1 SSW station are plotted in figure 5.

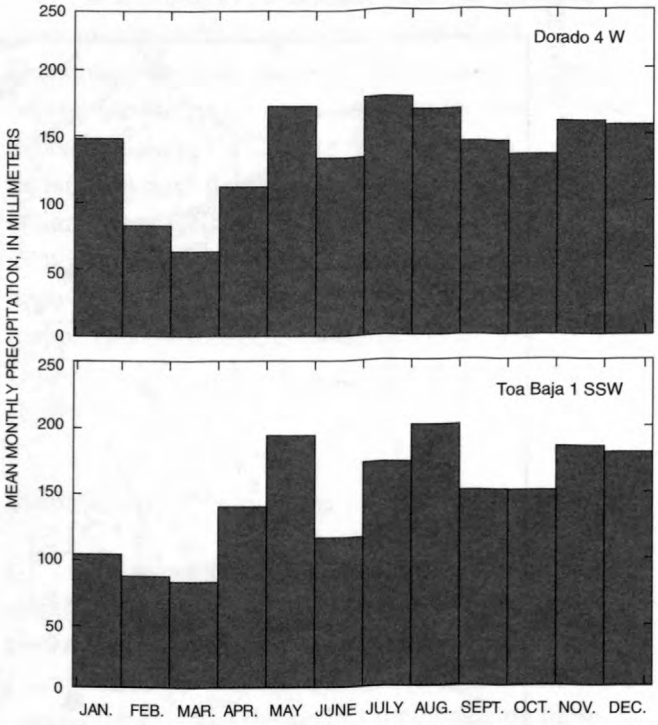

Figure 5. Graphs showing histograms of mean monthly precipitation at the Dorado 4 W station (Calvesbert, 1970) and the Toa Baja 1 SSW station (Southeast Regional Climate Center, unpublished data, 1995).

The USGS maintains factory-calibrated tipping-bucket precipitation gages at two gaging stations in the study area as part of the flood-alert network. Station 50046000, Río de la Plata at Highway 2 near Toa Alta, Puerto Rico, is near the center of the study area, whereas Station 50039500, Río Cibuco at Vega Baja, Puerto Rico, is on the western edge of the study area (fig. 4). Table 2 gives the measured month and annual precipitation at the USGS precipitation gage at Station 50046000, Río de la Plata at Highway 2 near Toa Alta, Puerto Rico, and at the precipitation gage maintained by Fernando Gómez-Gómez in Valparaíso, Cataño, Puerto Rico, for the period from January 1993 to December 1996. In general, the USGS tipping-bucket precipitation gages recorded less than the reported precipitation values given for the NOAA meteorological stations and the precipitation gage in Valparaíso during January 1993 to December 1996.

Table 1. Mean or normal precipitation reported in recent years for precipitation gages near Dorado, Puerto Rico

[na, not available]

Year	Annual precipitation, in millimeters				
	Dorado 2 WNW	Dorado 4 W	Candelaria, Toa Baja	Toa Baja 1 SSW	Valparaíso, Cataño
Mean for available years 1987 to 1996	1,728	na	2,028	1,802	1,501
Mean annual precipitation for 1951 to 1960 from Calvesbert (1970)	na	1,655	na	na	na
Climatological Normals for 1961 to 1990 (Southeast Regional Climate Center, unpublished data, 1995)	na	na	1,767	na	na

Table 2. Measured monthly and annual precipitation at the USGS factory-calibrated tipping bucket precipitation gage (at surface-water station 50046000) Río de la Plata at Highway 2 near Toa Alta, Puerto Rico (fig. 4), and a plastic 6-inch precipitation gage maintained by Fernando Gómez-Gómez in Valparaíso, Cataño (M5 in fig. 4).

Month	Precipitation, in millimeters			
	Calendar year			
	1993	1994	1995	1996
	Station 50046000, Río de la Plata at Highway 2 near Toa Alta			
January	37	69	101	121
February	14	11	68	77
March	48	23	22	4
April	158	104	36	31
May	155	61	49	22
June	74	54	203	43
July	28	67	74	15
August	58	98	52	22
September	184	64	167	312
October	92	101	124	130
November	121	89	108	163
December	44	38	88	107
Annual Total	1,014	779	1,092	1,047
	Valparaíso, Cataño			
January	84	114	121	173
February	40	20	107	41
March	58	42	29	80
April	296	142	24	173
May	266	75	128	196
June	130	147	110	213
July	237	92	179	97
August	28	108	121	90
September	116	115	330	332
October	101	57	102	68
November	118	149	161	263
December	103	53	100	71
Annual Total	1,578	1,116	1,514	1,797

Physiographic Features

The northern karst belt of Puerto Rico is known for its variety of karst landforms. These karst landforms have been described by Thorp (1934), Meyerhoff (1938), Doerr and Hoy (1957), Kaye (1957), Monroe (1964, 1966, 1974, 1976, 1979, 1980b), Thrailkill (1967), Miotke (1973), Sweeting (1973), Day (1978), Ireland (1979), Giusti (1978), Torres-González (1983), Troester and others (1984, 1987), and Troester (1992, 1994). Many different names have been proposed for these surface karst features. According to Sweeting (1973, p. 273), Troester and others (1987), and Troester (1992, 1994) there are two main types of humid tropical karst landforms: cone karst (also known as Kegelkarst, cockpit karst, and fengcong) and tower karst (also known as Turmkarst and fenglin). Cone karst is composed of many closely spaced cone- or tower-shaped hills separated by deep sinkholes with little level ground (Monroe, 1970). Tower karst is composed of isolated limestone hills separated by flat areas often covered with alluvium or other detrital sand (Monroe, 1970; Yuan, 1985; Williams, 1987). In Puerto Rico the tower karst is composed of limestone hills protruding through an aggraded surface of clastic sediments that buries the underlying karst topography. The tower karst in Puerto Rico is best developed on the Aymamón Limestone, but it is also developed on the Aguada Limestone and the Cibao Formation. In these areas the isolated hills of limestone usually rise about 30 m above the blanket sands. The sides are steep and rugged, but not vertical like the sides of some classic tower karst hills, so they are usually called mogotes, instead of towers. The study area is characterized by these limestone hills called mogotes, which are separated by relatively flat areas covered with blanket sands or other unconsolidated sediment.

Other significant geomorphic features of the study area include the Río Cibuco, the Río de la Plata, and the Río Bayamón, their alluviated valleys, and the coastal plain. When sea level was lower than it is today, as it was at various times during the Pleistocene Epoch, these rivers cut deep valleys near the coast. As the sea level rose, these valleys were filled with alluvial material transported by the rivers from the interior of the island. In addition, much of this alluvial material was transported along the coast by nearshore currents and was deposited along the coast. With the uplift of Puerto Rico and changing sea level, this material is now exposed above sea level along the coastal plain. The valley infilling is thickest and widest near the shoreline where the alluvial valley begins to merge with the coastal plain.

Streamflow Stations

The mean discharge at surface-water station 50046000 (fig. 4) for the period of record (1960 to 1996), is 7.31 m^3/s; however, the station is downstream from a public water-supply reservoir that regulates the discharge of the river. This station is near the center of the study area and has a drainage area of about 539 km^2. Station 50039500 (fig. 4) is 1 km downstream from the confluence of the Río Cibuco and the Río Indio and has a total drainage area of about 257 km^2, slightly less than half the drainage area of station 50046000. The mean discharge at station 50039500, for the period of record (1973 to 1996), is 3.46 m^3/s, which is slightly less than half of the mean discharge recorded at 50046000. Mean annual discharges for these two surface-water stations from 1987 to 1995 are listed in table 3. The drought in 1994 and the subsequent reduced releases from the dam upstream of station 50046000 resulted in the low mean discharges in that year.

Hydrogeology

The regional hydrogeology of the north coast limestone belt has been described by Giusti (1978), Heisel and others (1983), Troester and others (1987), Troester (1992, 1994), Rodríguez-Martínez (1995), Torres-González and others (1996), and Veve and Taggart (1996). Several USGS investigations have described in detail the hydrogeology of the upper aquifer in the Vega Alta quadrangle. The published investigations include Torres-González and Díaz (1984) and Gómez-Gómez and Torres-Sierra (1988). The report by Anderson (1976) on ground-water resources in the San Juan area contains some information about the geology and hydrology of the Bayamón quadrangle.

Table 3. Mean annual discharge at U.S. Geological Survey surface-water stations in the Dorado area, north-central Puerto Rico, water years 1987 to 1996

Water year[1]	Mean annual discharge, in cubic meters per second	
	Río de la Plata at Highway 2	Río Cibuco at Vega Baja
1987	7.19	5.47
1988	9.12	4.73
1989	6.09	2.81
1990	2.34	3.12
1991	6.63	3.91
1992	4.39	2.25
1993	6.06	4.45
1994	0.89	1.09
1995	3.00	1.94
1996	10.31	4.73
Mean discharge for the period of record[2]	7.31	3.46

[1] A water year extends from October 1 to September 30 of the following calendar year, for example, water year 1987 extends from October 1, 1986, to September 30, 1987.

[2] The period of record for the Río de la Plata at Highway 2 is from 1960 to 1996 and the period of record for the Río Cibuco at Vega Baja is from 1973 to 1996.

General information on selected wells in the Vega Alta and Bayamón quadrangles is presented in table 4. The location of these wells is shown in figure 4.

In the Vega Alta quadrangle and the southwest part of the Bayamón quadrangle, the upper aquifer is composed of the permeable parts of the Cibao Formation, the Aguada Limestone, the Aymamón Limestone, and the permeable parts of the overlying unconsolidated deposits. Vertical ground-water flow is limited by the relatively impermeable part of the Cibao Formation, which forms the lower boundary of the upper aquifer along the southern parts of the study area. In this southern part the saline-freshwater interface is not present. A lower artesian aquifer is present below the Cibao Formation, but it is not the subject of this report. Close to the coast, the saline-freshwater interface represents the lower boundary of the freshwater regime in the upper aquifer. A potentiometric-surface map of the upper aquifer in the Vega Alta quadrangle was produced by Torres-Sierra (1985). The direction of ground-water flow is generally northward toward the Atlantic Ocean.

The most permeable units of the upper aquifer thin toward the east and in the eastern part of the Bayamón quadrangle are above the water table. The permeable, producing zone of the upper aquifer in the eastern part of the Bayamón quadrangle exists within the Mucarabones Sand.

Gómez-Gómez and Torres-Sierra (1988) determined 34 values of transmissivity from aquifer tests in the Vega Alta quadrangle. Transmissivity at these sites ranged from 16 to over 14,000 m^2/day, and averaged about 2,500 m^2/day. In general, transmissivity is lowest in the Cibao Formation and highest in the Aymamón Limestone. Transmissivity values in the Aymamón Limestone are highest near the contact with the Aguada Limestone (for example, near wells 3 and 4 in fig. 4 and table 4), but are much lower near the coast.

Heisel and others (1983) produced an electrical analog ground-water flow model of the entire north coast aquifer. Gómez-Gómez and Torres-Sierra (1988) produced a digital ground-water model of the aquifer in the Vega Alta quadrangle. Some of the results in these studies were used in this report.

Table 4. General information on U.S. Geological Survey observation wells in the Dorado area and other wells that are discussed in this report

[PRASA, Puerto Rico Aqueduct and Sewer Authority; ADR, analog digital recorder; USGS, U.S. Geological Survey]

Well number	Local well name	USGS site ID	Land surface elevation, in meters	Distance to coast, in kilometers	Use of water and type of site and pump
1	Díaz, Gilberto (Barrio Espinosa)	182423066165000	70	7.54	Private water supply with submersible pump
2	Santa Elena (Fonalleda)	182554066152900	7	5.80	Private water supply with submersible pump
3	Maguayo #3 (PRASA)	182540066174100	28	5.40	PRASA public water supply with turbine pump
4	Gramas Lindas #4	182629066172800	17	3.58	Private water supply with submersible pump
5	Jardín Grama	182724066155100	3	2.96	Private water supply with submersible pump
6	USGS #01 Test Well (Toa Baja)	182654066150600	3.5	2.80	USGS observation well with ADR
7	San Antonio #2 (PRASA)	182707066164100	5	2.56	PRASA public water supply with turbine pump
8	Saro #1	182723066172400	9	1.98	Observation well with no pump
9	Dorado Beach No. 7	182746066170800	8	1.24	USGS observation well which had an ADR (this well has now been destroyed)
10	Dorado Airport	182804066173500	19	0.80	Unused private supply well with ADR
11	San Antonio 1 (USGS)	182657066162700	6	2.98	USGS observation well with ADR
12	San Antonio 2 (USGS)	182657066162702	6	2.98	USGS observation well with no pump
13	San Antonio 3 (USGS)	182657066162701	6	2.98	USGS observation well with ADR
14	Higuillar 1 (USGS)	182620066163400	12	4.00	USGS observation well with no pump
15	Higuillar 2 (USGS)	182620066163401	12	4.00	USGS observation well with no pump
16	Higuillar 3 (USGS)	182620066163402	12	4.00	USGS observation well with no pump
17	Higuillar 4 (USGS)	182620066163403	12	4.00	USGS observation well with ADR
18	Maguayo 1 (USGS)	182548066164400	12	4.84	USGS observation well with no pump
19	Maguayo 2 (USGS)	182548066164401	12	4.84	USGS observation well with ADR
20	Maguayo 3 (USGS)	182548066164402	12	4.84	USGS observation well with no pump
21	Santa Rosa 1 (USGS)	182526066165000	28	5.50	USGS observation well with no pump
22	Santa Rosa 2 (USGS)	182526066165001	28	5.50	USGS observation well with ADR
23	Fort Buchanan TW-1 (USGS)	182450066080500	15	3.42	USGS observation well with no pump
24	Campanillas Navy	182530066135400	4	4.88	USGS observation well with ADR
25	Monserrate TW-2	182655066142400	1	2.22	USGS observation well with ADR
26	Sabana Hoyos	182647066201700	15	3.94	USGS observation well with ADR
27	Ponderosa TW-1	182515066194000	30	6.25	USGS observation well with ADR
28	Pámpano No. 2	182330066185700	120	9.40	USGS observation well with ADR
29	Levittown No. 7	182623066111000	3	1.98	USGS observation well which had an ADR (this well has now been destroyed)
30	Buchanan Park Well	182441066082600	20	3.92	USGS observation well with ADR

Previous Estimates of Recharge

Ground water in the northern karst belt of Puerto Rico is recharged by infiltration from direct precipitation and losing streams. In mogote areas, recharge by direct infiltration through the relatively impermeable blanket sand deposits or the recrystallized or "case-hardened" limestone surface of the mogotes is limited (Monroe, 1966). The majority of recharge occurs from runoff during large rainfall events. Runoff from the mogote surface quickly flows into holes and solution channels around the base of the mogotes and recharges the aquifer (Miotke, 1973; Monroe, 1976; Day, 1978). Frequently, runoff from streams in the valleys between the mogotes surface also flows into sinkholes and recharges the aquifer. Water levels in wells in mogote areas have been observed to respond immediately to rainfall events (Michalski and Torlucci, 1988, 1989; Ewers and others, 1989).

Recharge through sinkholes in the mogote areas varies in both time and space. A spatial distribution of net recharge to the upper aquifer in the Vega Alta area, including the mogote areas, was presented by Gómez-Gómez and Torres-Sierra (1988) in a ground-water flow model report. Net recharge estimates summarized in this report ranged from 0 to 495 mm per year and averaged about 150 mm per year across the entire aquifer area. Estimates for mogote areas with internal drainage ranged from 250 to 495 mm per year. Net recharge estimates used by Gómez-Gómez and Torres-Sierra (1988) at specific well sites are given in table 5. Additional hydrogeologic data for these specific wells are also given in table 5.

Table 5. Estimates of net recharge and transmissivity and additional hydrogeologic data at selected well sites in the Dorado area, north-central Puerto Rico (based on Gómez-Gómez and Torres-Sierra, 1988)

[USGS, U.S. Geological Survey]

Well number	Well name	Land surface elevation, in meters	Average depth to the water table in meters for water year 1997[1]	Approximate thickness of unconsolidated material, in meters	Estimated net recharge, in millimeters per year[2]	Estimated transmissivity, in meter squared per day[3]
6	USGS #01 Test Well (Toa Baja)	3.5	2.90	27	99	930
10	Dorado Airport	19	17.73	17	99	370
11	San Antonio 1 (USGS)	6	5.12	15	99	2300
13	San Antonio 3 (USGS)	6	5.16	15	99	2300
17	Higuillar 4 (USGS)	12	10.37	23	371	2300
19	Maguayo 2 (USGS)	12	8.31	18	310	4600
22	Santa Rosa 2 (USGS)	28	19.05	19	371	2300
24	Campanillas Navy	4	4.62	27	99	2300
25	Monserrate TW-2	1	0.72	17	99	460
26	Sabana Hoyos	15	8.78	20	371	4600
27	Ponderosa TW-1	30	21.28	8	99	140
28	Pámpano No. 2	120	14.62	12	155	19

[1] Average depth to the water table in water year 1997 (October 1996 to September 1997). Data from U.S. Geological Survey (1998).

[2] The estimates of net recharge were derived from the Gómez-Gómez and Torres-Sierra (1988) ground-water flow model. Values for the well sites were obtained from simulated values at the grid cells containing the well sites.

[3] Values obtained from aquifer test from Gómez-Gómez and Torres-Sierra (1988).

METHODS

For this investigation, 13 wells were drilled into the upper aquifer in the Dorado area. Several representative new and existing wells were examined with borehole geophysical tools and geochemical methods. In addition, ground-water levels measured were used to calculate net recharge.

Drilling Method

Thirteen wells (wells 11 to 24, fig. 4) were drilled using a dual-tube, reverse air-rotary drilling system with an open-center bit. The dual-tube, open-center bit method uses a large compressor that forces air down the annulus between the dual-walls of the drill stem. The compressed air forces the drill cuttings, cores, and ground water into the open center of the bit where they are forced upward to the surface through the center of the drill stem. This method allows measurements of the specific conductance of the ground water without the interfering effects of drilling mud. Observation wells were constructed with 10-cm PVC casings.

Borehole Geophysical Methods

Electromagnetic and natural gamma radiation borehole geophysical tools were used in some of the deeper wells in the study area to determine the depth to bedrock and the saline-freshwater interface, to define changes in lithology, and to characterize the vertical distribution of hydraulic properties of the upper aquifer. In May 1995, 11 wells in the study area were logged with the EM 39 borehole conductivity and the Gamma 39 natural gamma radiation probes produced by Geonics.

The EM 39 borehole conductivity probe measures the apparent electrical conductivity of the sediment, rock, and water surrounding the well by using the inductive electromagnetic technique. The unit employs coaxial coil geometry and a coil spacing of 0.5 m. Values of apparent electrical conductivity were collected at 0.1-m intervals of depth. The specifications and theory of operation of the EM 39 borehole conductivity probe are described by McNeill (1986); field evaluations are presented by Taylor and others (1989), McNeill and others (1990), Mack (1993), and Williams and others (1993).

The apparent electrical conductivity of aquifer materials is primarily affected by the presence of clay minerals and the specific conductance of ground water. The specific conductance of water increases considerably with dissolved solids concentration. Metal near the borehole, such as a steel surface casing or metal lost from a drill bit, will be distinctly identified on the electromagnetic log as a sharply spiked, positive or negative response, which may extend beyond the normal scale. The electromagnetic logs of most wells in this study show evidence of metal interference from either pieces of metal worn from the drill bit or from the steel surface casing. Interference can range from a minor spike in the log trace to a complete obscuring of the log for intervals, such as the interval covered by a steel surface casing.

The Gamma 39 natural gamma radiation probe measures the naturally occurring gamma radiation in counts per second (cps) of the sediment, rock, and water surrounding the well. Gamma-emitting radioisotopes are natural products of radioactive decay and are usually concentrated in clays by the processes of adsorption and ion exchange. Therefore, clay-rich sediments are generally more radioactive than carbonate rocks and can be readily distinguished from carbonate rocks by use of this technique. By comparing the electromagnetic log, the natural gamma radiation log, and the cores and cuttings from the well, an investigator can determine whether a high electrically conductive zone is related to the presence of a clay layer or of a saline ground-water lens. More information on the specifications and operation of the Gamma 39 natural gamma radiation probe can be found in Mack (1993) and Williams and others (1993).

Geochemical Methods

Water samples were collected from nine existing production and abandoned wells in the Dorado area to determine the chemistry of the freshwater part of the upper aquifer. Abandoned wells were sampled with submersible pumps following the evacuation of at least three well volumes of water. Production wells were sampled using the available pump. The USGS #01 Test Well (Toa Baja) is completely screened from the water table to the bottom of the well and was sampled twice: once with the pump set about 2 m below the water table (about 6 m below land surface) and again with the pump set about 2 m from the bottom of the well (about 48 m below land surface).

Field measurements of temperature and specific conductance were made with a Yellow Springs Instrument Model 33 Salinity-Conductivity-Temperature meter. Field measurements of pH and alkalinity were conducted with an Orion pH meter using procedures described by Wood (1976).

Water samples were collected, filtered through a 0.45 µm filter, acidified with nitric acid, refrigerated to prevent precipitation, and analyzed in the laboratory for calcium, magnesium, sodium, potassium, silica, iron, and manganese. Water samples were collected, filtered through a 0.45 µm filter, refrigerated to prevent precipitation, and analyzed in the lab for chloride, sulfate, and fluoride. All laboratory analyses were performed by the USGS National Water Quality Laboratory using methods described by Fishman and Friedman (1989). Saturations indexes were calculated by the WATEQ4F water-quality computer model (Ball and Nordstrom, 1991).

THE GEOCHEMISTRY OF THE SALINE-FRESHWATER INTERFACE

The chemical analyses of 10 ground-water samples collected in the Dorado area are listed in table 6. These data were previously reported in Monell-González (1994). The specific conductance values of the samples listed in table 6 ranged from 470 µS/cm in well 2 to 3,600 µS/cm in the lower zone of well 6. Specific conductance values determined in wells drilled as part of this project ranged from 350 µS/cm in well 21 to about 45,000 µS/cm in well 11.

Specific conductance can be readily measured in the field, and dissolved-solids concentrations (in milligrams per liter) can be estimated by multiplying the specific conductance value (in microsiemens per centimeter) by a coefficient which usually ranges from 0.55 to 0.75 (Hem, 1985, p. 67). For example, using a coefficient of 0.59, the specific conductance value of 3,600 µS/cm obtained in well 6 is approximately equivalent to about 2,000 mg/L dissolved-solids concentration. For reference, typical ocean water has a dissolved-solids concentration of about 34,000 mg/L. Ground water with a specific conductance value of about 875 µS/cm typically will have a dissolved-solids concentration of about 500 mg/L, which is the U.S. Environmental Protection Agency secondary drinking water standard (U.S. House of Representatives, 1996).

All of the chemical analyses in table 6 were plotted in the Piper diagram in figure 6. The large arrows in figure 6 indicate the general trends in the chemical composition of water in the upper aquifer. As ground water flows through the upper aquifer and into the Atlantic Ocean, chemical reactions between the water and the minerals in the aquifer increase the dissolved-solids concentration and change the chemical composition of the water. The ground water in the aquifer changes from a calcium-bicarbonate type water in the recharge area (for example water samples from wells 1, 3, and 4) to a sodium-chloride type water near the coast (for example water samples from wells 5, 6, and 7). Additional details on the interpretation of Piper diagrams can be found in Piper (1944, 1953) and Briel (1993).

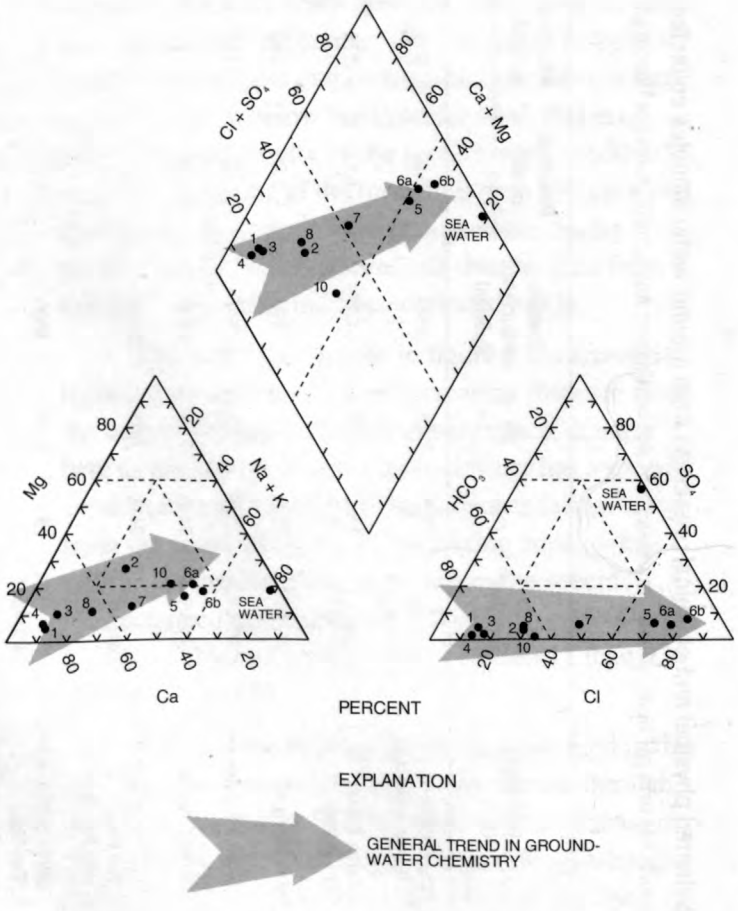

Figure 6. Piper diagram showing general trend in ground-water chemistry of sampled water in the Dorado area, north-central Puerto Rico (refer to fig. 4 for well locations).

Table 6. Selected physical and chemical properties from ground-water samples collected in the Dorado area, north-central Puerto Rico

[T, temperature; pH is in pH units; µS/cm, microsiemens per centimeter; mg/L, milligrams per liter; µg/L, micrograms per liter; SI_c, calcite saturation index; SI_a, aragonite saturation index]

Well number	Well name	Date sampled	T (°C)	pH	Specific conductance (µS/cm)	Dissolved oxygen	Alkalinity as $CaCO_3$	Ca	Mg	Na	Cl	SiO_2	Fe (µg/L)	SI_c	SI_a
						(mg/L)									
1	Díaz, Gilberto (Barrio Espinosa)	4/3/92	25.5	7.28	490	6.6	221	92	3.4	12	27	7.0	8	0.217	0.074
2	Santa Elena (Fonalleda)	3/23/92	25.2	7.53	470	6.1	278	75	26	48	86	30	71	0.435	0.292
3	Maguayo #3	3/25/92	25.6	7.10	500	5.0	246	94	7.3	16	35	7.2	9	0.088	-0.056
4	Gramas Lindas #4	3/24/92	25.3	7.08	500	7.2	255	110	5.4	13	28	7.0	14	0.141	-0.002
5	Jardín Gramas	3/25/92	24.6	7.20	1400	3.9	217	130	38	230	510	9.4	20	0.140	-0.004
6a	USGS #01 Test Well (Toa Baja) (near top of well)	4/2/92	26.9	7.05	2800	0.3	296	180	82	380	920	25	530	0.220	0.077
6b	USGS #01 Test Well (Toa Baja) (near bottom of well)	4/2/92	25.4	7.05	3600	0.5	237	210	88	520	1200	21	30	0.139	-0.004
7	San Antonio #2	3/30/92	25.0	7.15	700	1.3	232	96	14	75	150	9.0	6	0.076	-0.068
8	Saro #1	3/19/92	26.0	7.00	700	0.0	282	110	11	44	87	11	3000	0.086	-0.057
10	Dorado Airport	3/20/92	26.9	7.60	600	0.3	242	49	17	69	91	9.9	1500	0.308	0.165

The Piper diagram indicates that mixing (or hydrodynamic dispersion) with a sodium-chloride water, such as seawater has occurred. Possible sources of the sodium-chloride water include salt laden precipitation, the saline water that underlines the fresh water in the aquifer, and residual water left in the aquifer from deposition or when sea level was higher. Although it is not possible to differentiate between these sources of sodium-chloride water, a mass balance can be calculated assuming the chloride comes from modern seawater. The equation to calculate the chloride mass balance is

$$x = (Cl_{gw} - Cl_{fw})/(Cl_{sw} - Cl_{fw}), \quad (1)$$

where x is the mixing fraction, Cl_{gw} is the chloride concentration of the ground-water sample, Cl_{fw} is the lowest chloride concentration measured (27 mg/L in this case), and Cl_{sw} is the chloride concentration of the modern seawater (19,000 mg/L). Using this formula the percent of mixing ranges from 0 percent in well 1 to 6.2 percent in sample 6b taken from the bottom of well 6.

Saturation indexes were calculated using a digital water-quality model, WATEQ4F (Ball and Nordstrom, 1991). The saturation index is a measure of the departure from equilibrium of the water with respect to mineral phases. The saturation index (SI) is defined as

$$SI = \log(IAP/K_T), \quad (2)$$

where IAP is the ion activity product of the components of the mineral phase and K_T is the solid phase solubility equilibrium product at the specified temperature. A saturation index value of about zero indicates the water is in equilibrium or saturated with respect to the mineral phase, a saturation index less than zero indicates undersaturation (mineral dissolution is possible), and a saturation index greater than zero indicates oversaturation (mineral precipitation is possible). Saturation index estimates are usually considered to have an error of about $\pm$ 0.1. The results from WATEQ4F indicate that the ground water in most of the aquifer is near saturation with respect to aragonite and chalcedony (a cryptocrystalline variety of quartz) and slightly over saturated with calcite and quartz. The saturation indexes for calcite and aragonite for each sample are given in table 6.

HYDROGEOLOGIC FRAMEWORK

A total of 13 observation wells were constructed at five sites during 1994 and 1995. At each of the five sites, from one to four observation wells were completed. The 13 wells include wells 11 to 23 (table 7). Construction data for all of these wells are summarized in table 7. The lithologic description of the cores obtained from the four sites, San Antonio (wells 11 to 13), Higuillar (wells 14 to 17), Santa Rosa (wells 21 and 22), and Fort Buchanan (well 23), are summarized in tables 8 to 11. Electromagnetic and natural gamma geophysical logs from wells 11, 14, 20, and 21 are presented in figures 7a and 7b and the geophysical logs from wells 6 and 23 are presented in figure 8. In addition, the specific conductance of the ground water with depth obtained from these six sites during well construction are also presented in figures 7 and 8. Each of these graphs were plotted with the same scales for depth below land surface (0 to 160 m), electrical conductivity of the formation (0 to 600 mS/m), natural gamma of the formation (0 to 600 cps), and specific conductance of the ground water during pumping (0 to 50,000 µS/cm), so that the data from the different wells could be compared easily.

The individual graphs in figure 7 are arranged from left to right in order of decreasing distance from the ocean. The saline-freshwater interface, defined here as the point where the ground water has a specific conductance of 10,000 µS/cm, is deeper farther away from the coast. In addition, the mixing zone, defined here as the ground-water zone where the specific conductance ranges from 10,000 µS/cm to 45,000 µS/cm, is obviously more narrow at well 11 than it is at wells 14 and 20.

Much of the hydrogeologic data gathered in this study can be summarized by a cross section through the Dorado area (fig. 9). The cross section (shown in fig. 4) crosses the length of the Vega Alta quadrangle and passes through wells 11, 14, 20, and 21. The geologic data shown in this cross section are drawn from the geologic map of the Vega Alta quadrangle by Monroe (1963) and the lithologic descriptions in

Table 7. Observation wells installed in the Dorado area, north-central Puerto Rico, from 1993 to 1995

Well number[1]	Well name	USGS site ID	Screened interval, in meters below land surface	Total depth, in meters below land surface
11	San Antonio 1	182657066162700	82 to 85	91
12	San Antonio 2	182657066162702	61 to 67	73
13	San Antonio 3	182657066162701	20 to 23	24
14	Higuillar 1	182620066163400	143 to 146	149
15	Higuillar 2	182620066163401	115 to 118	121
16	Higuillar 3	182620066163402	76 to 82	85
17	Higuillar 4	182620066163403	24 to 27	30
18	Maguayo 1	182548066164400	122 to 125	128
19	Maguayo 2	182548066164401	29 to 32	34
20	Maguayo 3	182548066164402	33 to 36	37
21	Santa Rosa 1	182526066165000	91 to 98	101
22	Santa Rosa 2	182526066165001	37 to 40	43
23	Fort Buchanan TW-1	182450066080500	64 to 76	152

[1] Location of wells shown in figure 4.

tables 8 to 11. The water-table altitude was taken from Torres-Sierra (1985) with the addition of data from the new observation wells. The location of the saline-freshwater interface was drawn from specific conductance measurements obtained from ground-water samples collected during drilling and from data inferred from the electromagnetic and natural gamma geophysical logs (figs. 8, 9).

The hydraulic gradient of the water table reflects the difference in hydraulic conductivity of the geologic units in the area (fig. 9). The relatively flat gradient of the water table in the Aymamón Limestone is indicative of a highly transmissive unit. The slightly lower hydraulic conductivity of the Aguada Limestone is indicated by the steepening of the water-table gradient in this formation. The steepest water-table gradient is found in the Cibao Formation which has the lowest hydraulic conductivity of the geologic units present in the study area. This is accentuated by the fact that most aquifer recharge areas are underlain by both the Aguada Limestone and the upper member of the Cibao Formation. The Quebrada Arenas Limestone Member of the Cibao Formation has a higher hydraulic conductivity and a milder water-table gradient than the upper member of the Cibao Formation. In this cross section, ground water in the Quebrada Arenas Limestone Member may be flowing east, following the direction of the Río Lajas as documented by Gómez-Gómez and Torres-Sierra (1988). It appears that there is relatively little ground-water flow north from the Quebrada Arenas Limestone Member through the less permeable upper member of the Cibao Formation to the upper aquifer in the Aguada Limestone and Aymamón Limestone. The top of the Cibao Formation represents the base of the upper aquifer in the southern half of the study area.

In the northern half of the study area, the saline-freshwater interface forms the base of the freshwater aquifer in the Aguada Limestone and Aymamón Limestone (fig. 9). It is important to note that all wells in PRASA's San Antonio well field and some wells in PRASA's Maguayo well field are completed near the saline-freshwater interface.

Table 8. Lithologic description of cores obtained at the San Antonio drill site, wells 11 to 13, Dorado area, Puerto Rico

Depth below land surface (in meters)	Description
0 to 1	Moderate yellowish brown (10YR5/4)[1], loose topsoil, with 5 to 10 percent pebbles. Iron stained clay and silt with some very fine sand.
1 to 13	Alluvium, ancient deltaic, and mud-flat deposits consisting of mottled moderate yellowish brown to moderate reddish brown (10YR4/6) clay. Some clay nodules are light gray (N8) on the inside. Calcareous material, iron staining, and manganese nodules are common. Clay balls from near water table (5 to 6 meters) are stiff.
13 to 15	Intermixed clay and limestone. The limestone is fragmented and highly weathered with pieces less than 10 millimeters in size and with hematite veinlets.
15 to 37	Aymamón Limestone. Packstone with minor clay and minor coarse sand. Highly crystalline, fossiliferous (gastropods and corals), highly weathered, iron stained limestone with small clay-filled cavities (clay filled) about 3 to 6 millimeters in size.
37 to 51	Alternating layers of dark yellowish orange (10YR6/6) calcareous clay wackestone and packstone. Returns are fragmented into pieces only 5 to 10 millimeters in size.
51 to 91	Aguada Limestone. Chalky limestone with little or no clay. Microcrystalline powdery limestone or chalk, minor fossils (corals and pelecypods). Recovery averages between 5 to 10 millimeters and up to 25 millimeters. Color ranges from white (N9) to very pale orange (10YR8/2). There are very few cavities. The rock is well cemented in places. At 80 meters in depth, 50 to 75 millimeter pieces of core were recovered with trace fossil corals.

[1] Color codes are according to Goddard and others (1948).

Table 9. Lithologic description of cores obtained at the Higuillar drill site, wells 14 to 17, Dorado area, Puerto Rico

Depth below land surface (in meters)	Description
0 to 1	Clayey, light brown (5YR5/6)[1] topsoil, with moderate reddish brown (10YR4/6) striations. The soil is friable and contains trace pebbles.
1 to 16	Alluvium and river terrace deposits. Mottled dark yellowish orange (10YR6/6) to moderate yellowish brown (10YR5/4) clay with 25 millimeter diameter nodules of moist light olive gray (5Y6/1) clay.
16 to 23	Clay, same as above, but with 10 to 25 millimeter subangular indurated fossiliferous limestone.
23 to 27	Aymamón Limestone. White to very pale orange (10YR8/2), very hard packstone with abundant fossils (gastropods and corals), secondary calcite, and small cavities (about 3 millimeters in diameter) common.
27 to 99	Aguada Limestone. White, hard, chalky limestone, with abundant fossils (gastropods, corals, and pelecypods) and trace sand and clay. The limestone is recemented in areas.
99 to 149	Upper member of the Cibao Formation. Highly weathered, light gray (N7), medium hard calcareous claystone and wackestone, with skeletal debris. Medium to coarse grained sand is common, with alternating beds of well cemented fossiliferous (pelecypods, gastropods, and corals) claystone and chalky claystone. At 136 meters, sand increases and cementation decreases.
149 to 152	Miranda Sand Member of the Cibao Formation. Greenish gray (5G6/1) medium to coarse grained sand.

[1] Color codes are according to Goddard and others (1948).

Table 10. Lithologic description of cores obtained at the Santa Rosa drill site, wells 21 and 22, Dorado area, Puerto Rico

Depth below land surface (in meters)	Description
0 to 1	Mottled moderate yellowish brown (10YR5/4)[1] to dark yellowish orange (10YR6/6) clayey topsoil. The soil is stiff, moderately cohesive (almost friable), and contains manganese nodules.
1 to 19	Alluvium. Moderate yellowish brown (10YR5/4) clay with reddish hue (10YR4/6). Forms 10 to 25 millimeter clay balls. Manganese nodules are common. A trace amount of medium to coarse grained sand is present. At 18 meters, a few limestone cobbles are present.
19 to 22	Aguada Limestone. Moderate brown (5YR4/4), indurated microcrystalline limestone with soft chalky zones, several clay layers (less than 150 millimeters) and trace pelecypod fossils. The limestone is highly weathered and has pitted surfaces.
22 to 30	Aguada Limestone. Clayey, highly weathered limestone with trace fossil corals.
30 to 84	Aguada Limestone. Chalky, white to very pale orange (10YR8/2) packstone, with abundant fossils (gastropods, corals, and pelecypods). The limestone is very hard, but highly weathered, with free secondary calcite crystals. A layer of clayey wackestone, with some coarse sand (5 to 10 percent) is at 69 to 71 meters.
84 to 107	Upper member of the Cibao Formation. A well cemented, very pale orange to light gray (N7) clayey wackestone, with occasional greenish gray hues, abundant fossils (pelecypods and corals), and common medium to coarse grained sand.
107 to 111	Upper member of the Cibao Formation. Greenish gray (5GY6/1), friable sandy clay with mottled brown striations. Mostly very fine- to fine-grained sand, but coarse to very coarse grained locally.
111 to 112	Olive gray (5Y4/1) to greenish gray (5GY6/1) calcareous clay and clay.
112 to 116	Fossiliferous (gastropods and pelecypods), rubbly limestone, indurated or well cemented in places, with fine- to medium-grained sand common and some pebbles. The limestone was deposed in a high energy reef environment.
116 to 122	Alternating layers of sandy clay and calcareous clay, with localized sand.

[1] Color codes are according to Goddard and others (1948).

Table 11. Lithologic description of cores obtained at the Fort Buchanan drill site, well 23, Dorado area, Puerto Rico

Depth below land surface (in meters)	Description
0 to 18	No core recovery.
18 to 43	Mottled light olive gray (5Y6/1)[1] to grayish yellow green (5GY7/2) clay and silt with about 20 percent medium to coarse angular sand. The color changes to light brown at about 24 meters. At 29 meters, the percent of clay decreases and the percent of sand increases. The sand is friable. At 35 meters the percent of clay and silt increases.
43 to 55	Minor core recovery of fused silt, sand, and clay. The pieces of core are about 50 millimeters, and up to 100 millimeters, in length.
55 to 58	Mottled, olive gray, greenish gray, and light brown clay with iron stains.
58 to 67	Fine grained sand with minor pebbles and gravel. Hard drilling from 58 to 59 meters. Increasing coarse material at 59 meters with minor fine grained material. Clay layer at 66 meters.
67 to 71	Sand and clay.
71 to 79	Clean, greenish gray (5GY6/1), subangular fine- to medium-grained sand, some very fine grained sand, increasing grain size at 73 meters. Medium to coarse grained sand composed of quartz and feldspar with minor mafic minerals. Minor clay layer at 78 meters.
79 to 82	No core recovery.
82 to 91	Sand and clay with increased clay at 84 meters and increased sand at 85 meters. Clay layer at 90 meters.
91 to 107	Fine- to medium-grained sand with minor clay. At 102 meters there is an increase in fine sand. At 104 meters there is an increase in grain size to coarse sand and pebbles.
107 to 116	Mottled moderate brown clay with iron stains and minor sand.
116 to 131	Fine- to very coarse-grained, predominantly medium-grained sand, some angular to subangular pebbles, greenish hue - possibly glauconite. Slight increase in fines, sticky clay increase in very fine grained sand at 126 meters.
131 to 137	Mottled greenish gray and light brown clay with some sand.
137 to 144	Sand and clay with some pebbles.
144 to 149	Clay with minor sand and pebbles.
149 to 152	Coarse grained sand and pebbles with minor clay.

[1] Color codes are according to Goddard and others (1948).

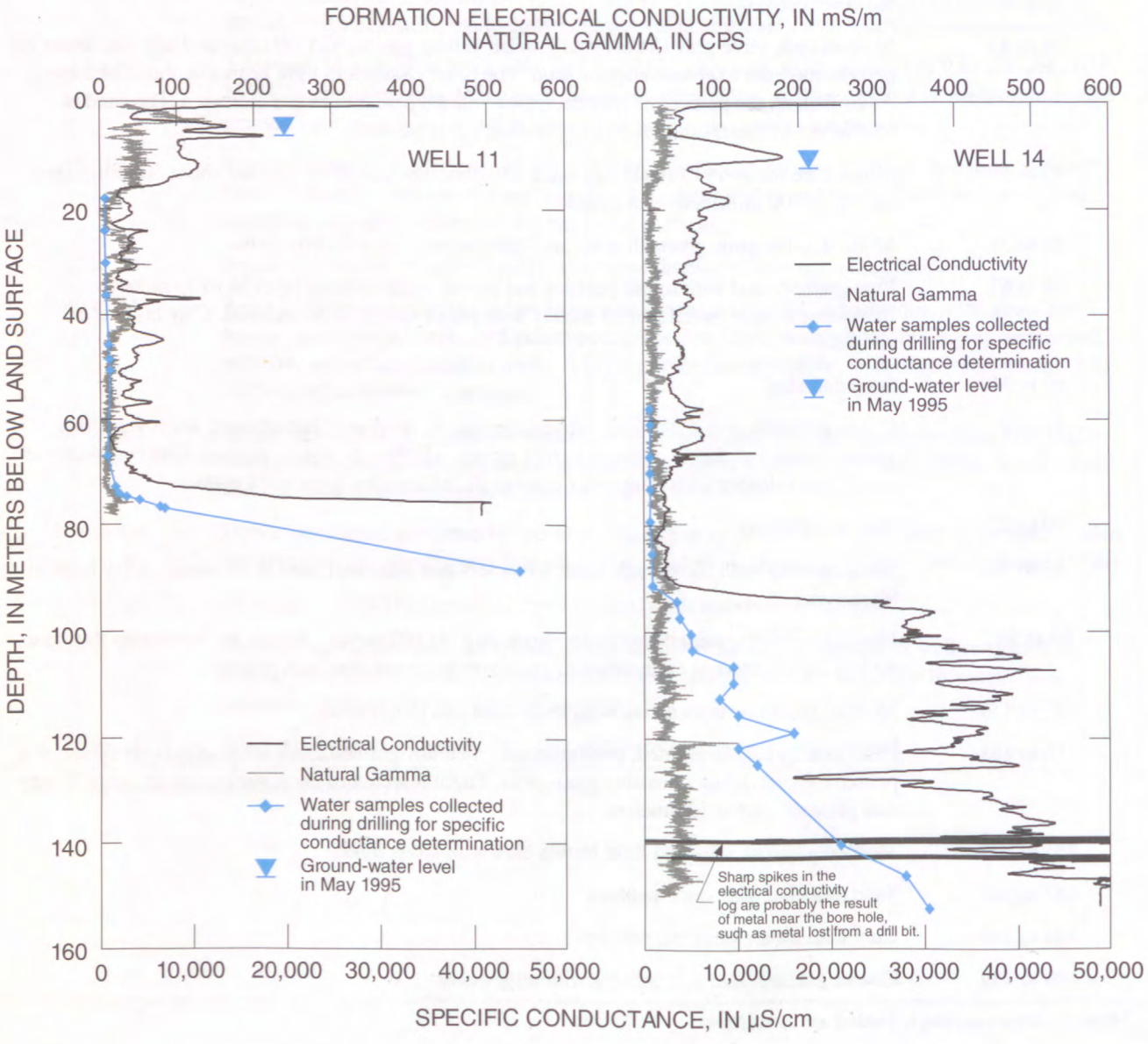

Figure 7a. Values of specific conductance of ground-water samples collected during drilling (December 1993 for well 11 and September 1994 for well 14) and natural gamma and formation electrical conductivity geophysical logs obtained in May 1995 from observation wells 11 and 14 in the Dorado area, north-central Puerto Rico (refer to fig. 4 for well locations). The wells are cased with PVC with a steel surface casing. Casing details are in table 7. Sharp spikes in the electrical conductivity log are probably the result of metal near the bore hole, such as steel surface casing or metal lost from a drill bit.

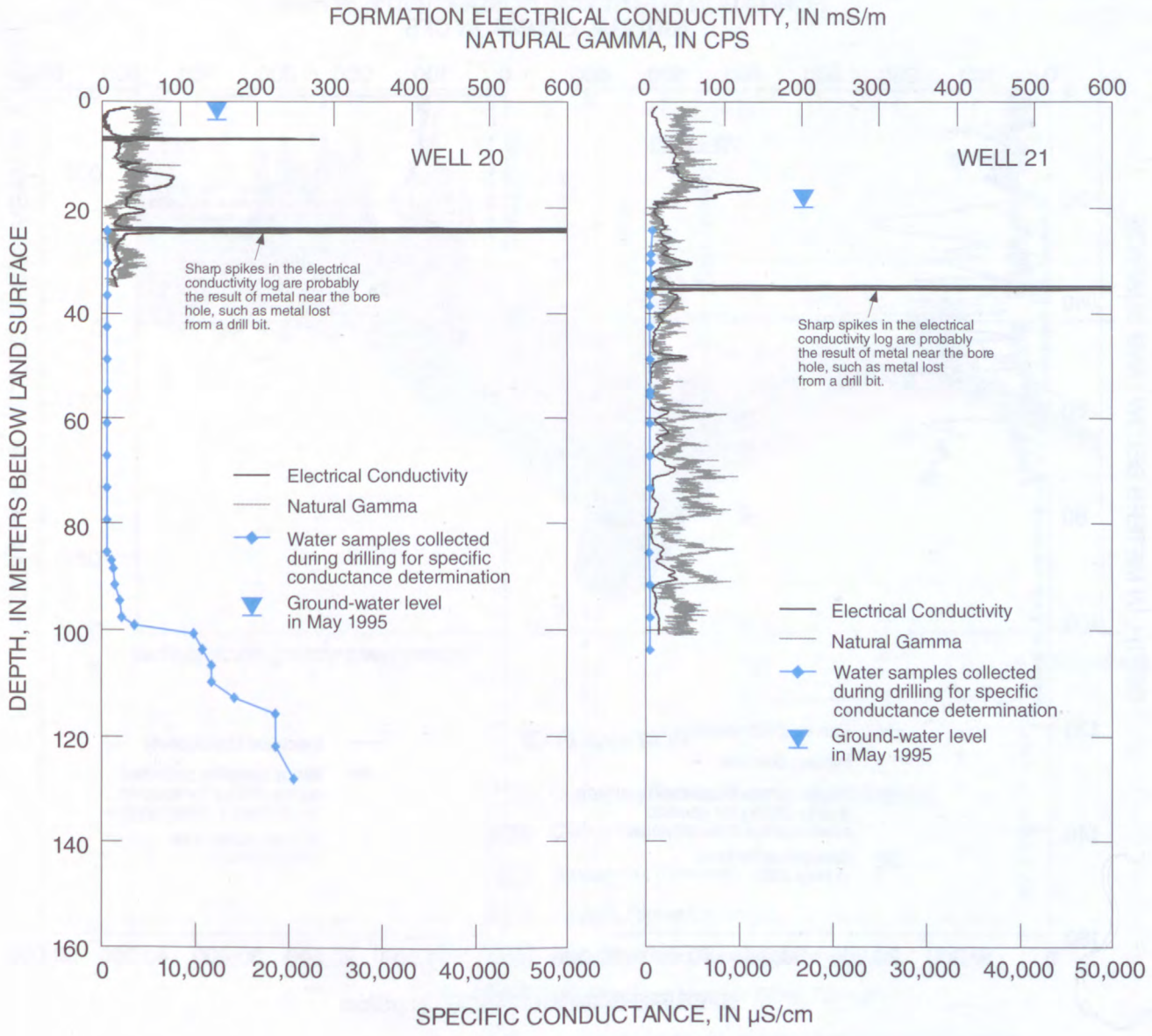

Figure 7b. Values of specific conductance of ground-water samples collected during drilling (February 1995 for well 20 and December 1994 for well 21) and natural gamma and formation electrical conductivity geophysical logs obtained in May 1995 from observation wells 20 and 21 in the Dorado area, north-central Puerto Rico (refer to fig. 4 for well locations). The wells are cased with PVC with a steel surface casing. Casing details are in table 7. Sharp spikes in the electrical conductivity log are probably the result of metal near the bore hole, such as steel surface casing or metal lost from a drill bit.

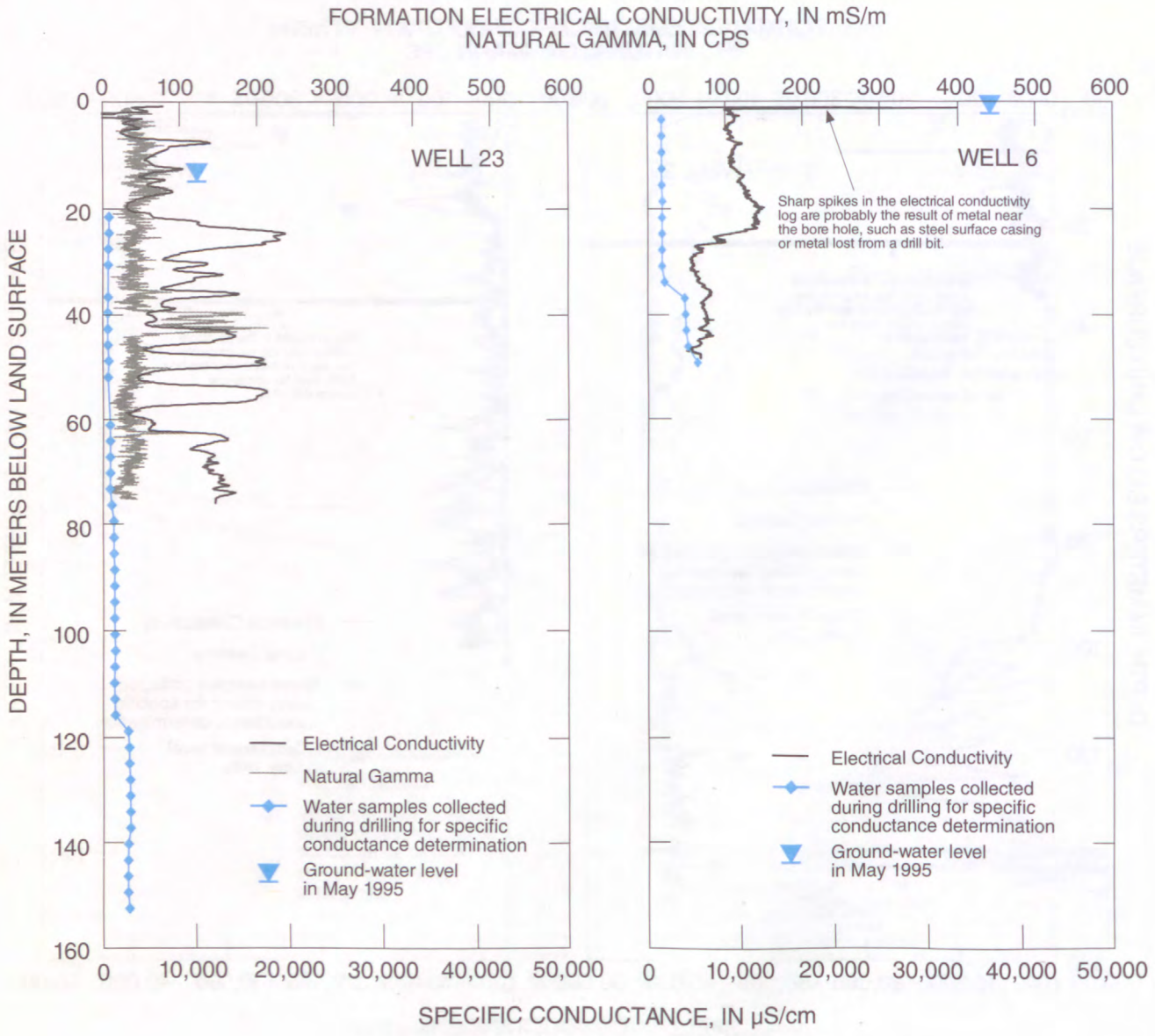

Figure 8. Values of specific conductance of ground-water samples collected during drilling (October 1984 for well 23 and June 1994 for well 6) and natural gamma and formation electrical conductivity geophysical logs obtained in May 1995 from observation wells 23 and 6 in the Dorado area, north-central Puerto Rico (refer to fig. 4 for well locations). The wells are cased with PVC with a steel surface casing. The casing in Well 6 is slotted from 8 to 50 meters below land surface. Casing details for well 23 are in table 7. Sharp spikes in the electrical conductivity log are probably the result of metal near the bore hole, such as steel surface casing or metal lost from a drill bit.

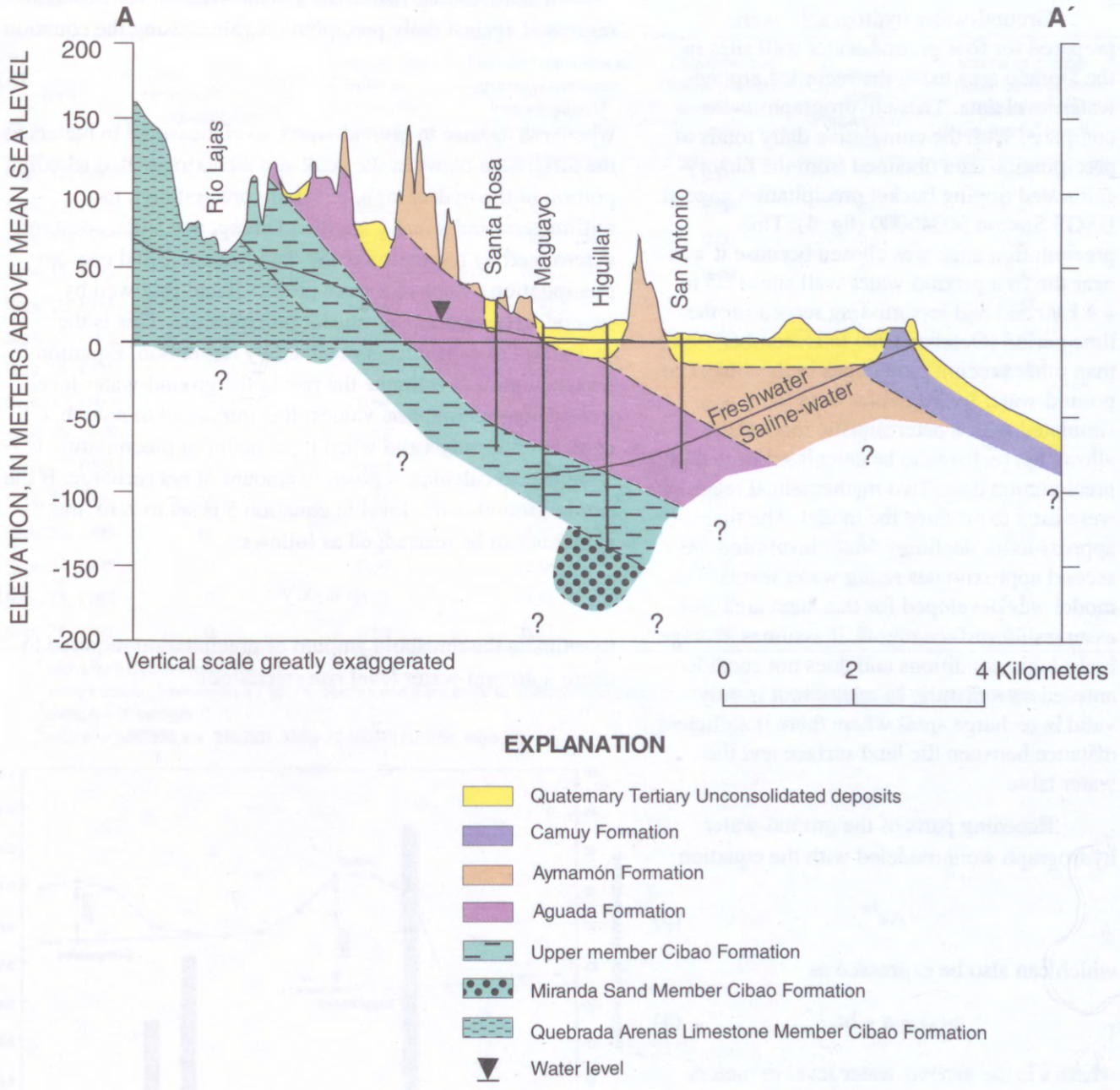

Figure 9. Cross section A-A' showing the approximate location of the saline-freshwater interface in the Dorado area, north-central Puerto Rico. The data for this cross section were adapted from Monroe (1963) and Torres-Sierra (1985) with additional data collected from the U.S. Geological Survey observation wells drilled from 1993 to 1995.

CALCULATION OF NET RECHARGE FROM PRECIPITATION AND GROUND-WATER LEVELS

Ground-water hydrographs were prepared for four ground-water well sites in the Dorado area using the recorded ground-water level data. These hydrographs were compared with the cumulative daily totals of precipitation data obtained from the factory-calibrated tipping bucket precipitation gage at USGS Station 50046000 (fig. 4). This precipitation gage was chosen because it was near the four ground-water well sites (2.5 to 4.4 km) and had less missing record for the time period (October 1994 to December 1996) than other precipitation gages in the area. The ground-water hydrographs were then simulated with a deterministic model that allows net recharge to be calculated from daily precipitation data. Two mathematical relations were used to produce the model. The first approximates declining water levels and the second approximates rising water levels. The model was developed for this karst area and assumes no surface runoff. It assumes average hydrologic conditions and does not consider antecedent moisture. In addition, it is only valid in recharge areas where there is sufficient distance between the land surface and the water table.

Receding parts of the ground-water hydrograph were modeled with the equation

$$s = Ae^{bt}, \tag{3}$$

which can also be expressed as

$$\ln(s) = a + bt, \tag{4}$$

where s is the ground-water level in meters above mean sea level, t is time in days, and a and b are the intercept and slope constants determined by linear regression of ground-water level against time (equation 4) and a is ln(A). This is the first of two sets of constants obtained by regression. Trends in declining water levels were extrapolated, as shown in figure 10, for periods of rising water levels by multiplying the receding ground-water level from the previous days by e^b. The rise from an individual recharge event was computed as the difference between the peak and the extrapolated receding part of the hydrograph.

The measured rise in the ground-water level was then regressed against daily precipitation values using the equation

$$r = x + yp, \tag{5}$$

where r is the rise in ground-water level measured in meters as the difference between the peak and the extrapolated receding portion of the hydrograph, p is daily precipitation in millimeters, and x and y are the intercept and slope constants determined by regression using data from selected one-day precipitation events that were preceded and followed by several days without significant precipitation. This is the second set of coefficients obtained by regression. Equation 5 was then used to estimate the rise in the ground-water level from daily precipitation values. It is important to note that equation 5 is only valid when the amount of precipitation is sufficient to calculate a positive amount of net recharge. If the rise in ground-water level in equation 5 is set to zero, the equation can be rearranged as follows:

$$p = -x/y \tag{6}$$

to estimate the threshold amount of precipitation required to cause a ground-water level rise (recharge).

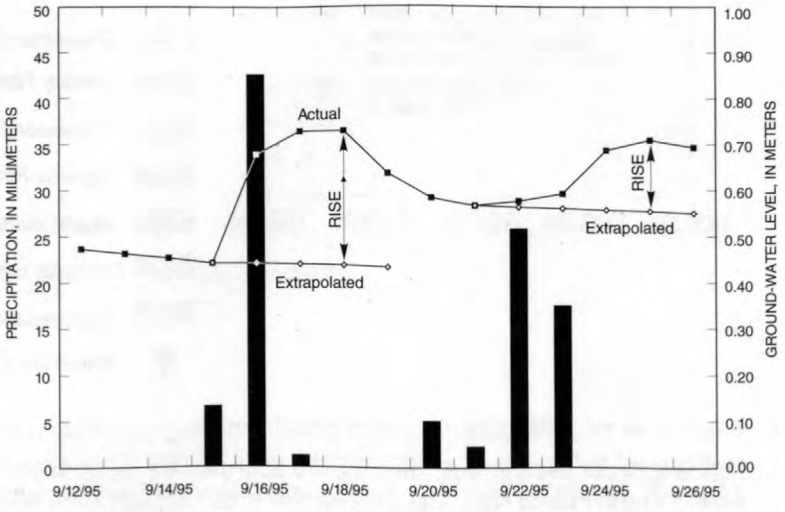

Figure 10. Graph showing example of method used to extrapolate receding portions of ground-water hydrographs and measure rise. The precipitation data are from USGS Station 50046000 and the ground-water data are from observation well 11 (refer to fig. 4 for well location). The data used to prepare this figure are in tables 12 and 13.

Table 12. Data used to prepare the example of method used to extrapolate receding portions of ground-water hydrographs and measure rise (fig. 10). The precipitation data are from USGS Station 50046000 and the ground-water data are from observation well 11 (refer to fig. 4 for well location).

[mm, millimeters; masl, meters above mean sea level; nd, not determined]

Date	Daily precipitation from USGS Station 50046000 (mm)	Ground-water level at San Antonio 1 (masl)	Projected recession in ground-water levels from equation 3[1] (masl)	Calculated net rise in ground-water level[2] (m)	Net recharge from equation 8[3] (mm)	Simulated ground-water levels at San Antonio 1 from equation 7[4] (masl)
Sept. 12, 1995	0	0.47	nd	0.00	0	0.47
Sept. 13, 1995	0	0.46	nd	0.00	0	0.47
Sept. 14, 1995	0	0.46	nd	0.00	0	0.47
Sept. 15, 1995	7	0.44	0.44	0.00	0	0.46
Sept. 16, 1995	43	0.68	0.44	0.16	16	0.63
Sept. 17, 1995	1	0.73	0.44	0.00	0	0.63
Sept. 18, 1995	0	0.73	0.44	0.00	0	0.62
Sept. 19, 1995	0	0.64	0.43	0.00	0	0.62
Sept. 20, 1995	5	0.58	nd	0.00	0	0.61
Sept. 21, 1995	2	0.57	0.57	0.00	0	0.61
Sept. 22, 1995	26	0.58	0.56	0.08	8	0.69
Sept. 23, 1995	18	0.59	0.56	0.04	4	0.72
Sept. 24, 1995	0	0.69	0.56	0.00	0	0.72
Sept. 25, 1995	0	0.71	0.55	0.00	0	0.71
Sept. 26, 1995	0	0.69	0.55	0.00	0	0.71

[1] with $e^b = 0.993598$ (from table 13)

[2] using equation 5 whenever $x + yp > 0$, where x and y are equal to -0.053937 and 0.005118 (from table 13) and p is precipitation in millimeters

[3] using $\phi = 10$ percent

[4] with $e^b = 0.993598$, $x = -0.053937$, and $y = 0.005118$ (all from table 13)

Table 13. Dates of available ground-water data and regression coefficients for selected observation wells in the Dorado area, north-central Puerto Rico

Well number	Well name	Dates of available ground-water data	Number of missing days	First regression[1] (regression for the receding limb of the hydrograph)				Second regression[2] (regression for the rising limb of the hydrograph)				
				n (number of days from Feb. 23 to June 12, 1996)	Regression coefficient b	e^b	r^2	n (number of storms)	Regression coefficient x	Regression coefficient y	Estimated threshold amount of precipitation required to cause a rise in the ground-water level, -x/y, in millimeters	r^2
11	San Antonio 1 (USGS)	October 20, 1994, to November 26, 1996	0	111	-0.006422	0.993598	0.83	22	-0.053937	0.005118	11	0.91
13	San Antonio 3 (USGS)	October 20, 1994, to November 26, 1996	22	111	-0.007494	0.992533	0.95	24	-0.057568	0.005327	11	0.94
17	Higuillar 4 (USGS)	January 23, 1995, to November 20, 1996	0	111	-0.003358	0.996647	0.93	20	-0.042161	0.004634	9	0.95
19	Maguayo 2 (USGS)	June 23, 1995, to November 18, 1996	0	111	-0.001505	0.998495	0.93	18	-0.063831	0.005946	11	0.96
22	Santa Rosa 2 (USGS)	June 7, 1995, to November 18, 1996	52	111	-0.000632	0.999367	0.94	15	-0.074029	0.005260	14	0.97

[1] equation 4
[2] equation 5

These two mathematical relations (equations 3 and 5) were combined to form the following deterministic model

$$\text{if } x + yp > 0 \text{ then } s_{i+1} = s_i + (x + yp) \text{ else } s_{i+1} = s_i \cdot e^b, \quad (7)$$

where s_i is the ground-water level on day "i" and s_{i+1} is the ground-water level on the next day, day "i+1." This model estimates the ground-water level on any given day based on daily precipitation values and an initial ground-water level. Examples of an actual ground-water hydrograph and a simulated hydrograph are given in figure 11.

Net recharge can be calculated using the equation

$$R = r \cdot \phi \quad (8)$$

where R is net recharge, r is the ground-water level rise calculated by equation 5, and ϕ is porosity. Again, this equation is only valid when the calculated rise in ground-water level (difference between the measured ground-water level and the extrapolated receding hydrograph) is positive. The total net recharge for a given period can be obtained by summing the individual net recharge values.

The cumulative daily total precipitation data from the USGS tipping bucket precipitation gage at station 50046000 are shown in figure 12a for October 1, 1995, to December 31, 1997. Precipitation totals of 1,092 and 1,047 mm were recorded at this site for calendar years 1995 and 1996, respectively. These precipitation amounts are about 60 percent of the normal precipitation reported at the long-term NOAA precipitation gage in Candelaria, Toa Baja (table 1 and site M4 in fig. 1) for 1961 to 1990 and indicate the relatively drier than average conditions which occurred during 1994 to 1996. It is possible that some of the difference between the USGS gage in 1995 and 1996 and the precipitation reported by NOAA for their gage from 1961 to 1990 is not the result of drier conditions, but the result of underreporting by the USGS gage. To attribute all of the difference between the USGS gage and the NOAA gage to underreporting is considered to be a worse-case scenario.

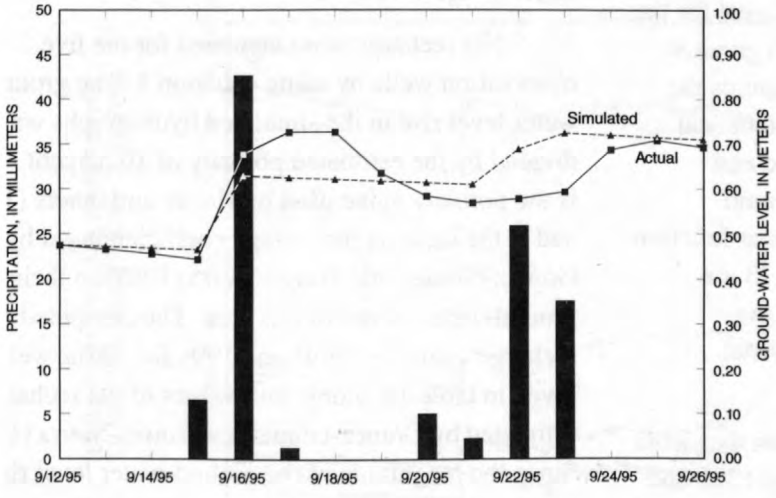

Figure 11. Graph showing an example of actual and simulated hydrographs. The precipitation data are from USGS Station 50046000 and the ground-water data are from observation well 11 (refer to fig. 4 for well location).

Two large storms with daily totals of 87 and 55 mm of rain occurred in June 1997 (fig. 12a). Hurricane Luis and Hurricane Marilyn (Torres-Sierra, 1997b) passed close to the island on September 6 and 16, 1995, respectively. These two Hurricanes produced about 47 and 51 mm, respectively, of precipitation in the Dorado area. Hurricane Hortense struck the island on September 10, 1996 (Gómez-Gómez, 1997; Torres-Sierra, 1997a). This hurricane had a major impact on the island and produced 252 mm of precipitation in the Dorado area. Results of many small storms are indicated on the graph as almost indistinguishable small offsets.

Larger scale rainfall patterns are also shown in figure 12a. From October 1, 1994, to June 1, 1995, precipitation fell at an average rate of 65 mm per month. From June 1, 1995, to March 1, 1996, precipitation fell at an average rate of 110 mm per month. This greater than normal rainfall rate was followed by a noticeable dry period during the six months (March 1 to September 1, 1996) preceding Hurricane Luis. During this dry period rain fell at a rate of about 25 mm per month. From September 1 to December 31, 1996, rain fell at a rate of 180 mm per month, although much of this fell during Hurricane Hortense.

Ground-water levels from October 1, 1994, to December 31, 1996, for observation wells 11, 13, 17, 19, and 22 are also shown in figure 12b. Water levels in these wells can be compared with the cumulative precipitation graph for the same time period in figure 12a in order to determine the relation between precipitation and water-level changes.

Ground-water recharge from precipitation of Hurricanes Luis and Marilyn, on September 6 and 16, 1995, caused two relatively small rises in ground-water levels in the study area (fig. 12b). However, the recharge from Hurricane Hortense on September 10, 1996, significantly raised ground-water levels that persisted for months in the area. The drier periods of March to August 1995 and March to May 1996 reflect declining water levels in figure 12b.

The slow decline in ground-water levels from February 23 to June 12, 1996 (111 days), was used to calculate the b coefficient defined in equation 3 (page 26). Computed values for this coefficient and other regression coefficient values for observation wells 11, 13, 17, 19, and 22 are given in table 13. These values were used to determine the rise in ground-water levels for about 20 significant storms during the study period. These data were then used to determine the regression coefficients x and y in equation 5. Values for n (number of significant storms), x, y, -x/y (the estimated precipitation with no net recharge), and other regression coefficients for the second set of regression equations are also given in table 13. A regression coefficient that measures the deviation of the data from the linearized statistical function used to represent it was computed and summarized in table 13 under the "r^2" column. If "r^2" equals one, the deviation from a linear function is zero. The values of "r^2" shown in table 13 are indicative of a good linear relationship of the data represented by the linear statistical model (equation 7).

As mentioned above, the precipitation data from the USGS gage at station 50046000 during 1995 and 1996 is about 60 percent of the normal precipitation reported at the long-term (1961 to 1990) NOAA precipitation gage in Candelaria, Toa Baja. If this difference is not a result of drier conditions, but a result of underreporting by the USGS gage, then the values of y and -x/y reported in table 13 are incorrect. Assuming the worse-case scenario (the USGS gage reports only 60 percent of the actual precipitation), then the values of y should be decreased by multiplying the reported values by 0.60. Consequently, the values reported for -x/y should be increased by dividing the reported values by 0.60. The range of values of -x/y would change from 9 to 14 mm to 15 to 23 mm.

Simulated ground-water hydrographs were produced for the five observation wells using the linear statistical model (equation 7), precipitation values from USGS tipping bucket precipitation gage station 50046000, and the values of the regression coefficients (b, x, and y) given in table 13. The ground-water elevation on October 1, 1994, was used as a starting point for each simulated hydrograph. Since this date was prior to continuous ground-water monitoring at these sites, the starting point was adjusted until a match was produced for the first ground-water level data point. The simulated ground-water hydrographs from October 1, 1994, to December 31, 1996, for observation wells 11, 13, 17, 19, and 22 are shown in figure 12c. These simulated hydrographs can be compared with the cumulative precipitation graph for the same time period in figure 12a and the actual ground-water levels for the same wells in figure 12b.

Net recharge was calculated for the five observation wells by using equation 8. The ground-water level rise in the simulated hydrographs was divided by the estimated porosity of 10 percent. This is the porosity value used by Heisel and others (1983) and is the same as the storage coefficient used by Gómez-Gómez and Torres-Sierra (1988) in their ground-water model of this area. The computed net recharge values for 1995 and 1996 for all the wells are given in table 14, along with values of net recharge estimated by Gómez-Gómez and Torres-Sierra (1988). Since the magnitude of the ground-water level rise in the simulated hydrographs is the same as that measured in the observation wells (fig. 12), underreporting by the USGS precipitation gage at station 50046000 does not affect the computed values of net recharge given in table 14.

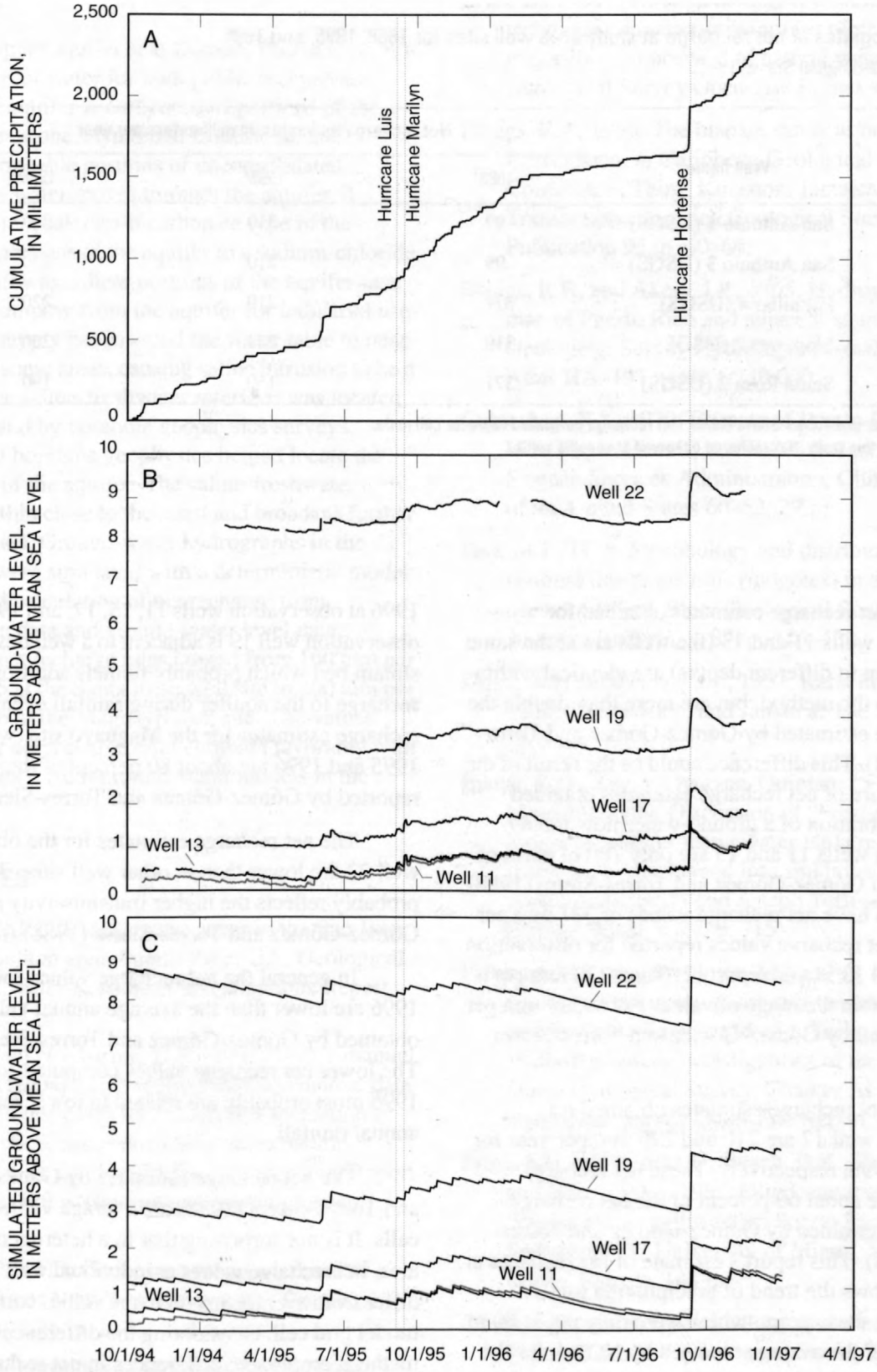

Figure 12. (A) Cumulative precipitation at USGS station 50046000; (B) ground-water levels at observation wells 11, 13, 17, 19, and 22; and (C) simulated ground-water hydrographs at observation wells 11, 13, 17, 19, and 22 in the Dorado area, north-central Puerto Rico (refer to fig. 4 for locations).

Table 14. Estimates of net recharge at study area well sites for 1988, 1995, and 1996

[USGS, U.S. Geological Survey]

Well number	Well name	Net recharge estimates, in millimeters per year		
		1988[1]	1995[2]	1996[2]
11	San Antonio 1 (USGS)	99	210	230
13	San Antonio 3 (USGS)	99	210	230
17	Higuillar 4 (USGS)	371	210	220
19	Maguayo 2 (USGS)	310	240	260
22	Santa Rosa 2 (USGS)	371	160	190

[1] Gómez-Gómez and Torres-Sierra (1988). Net recharge calibrated value for cell node.

[2] Results from this study. Net recharge observed at specific wells.

The net recharge estimates obtained for observation wells 11 and 13 (the wells are at the same site, but open to different depths) are identical within the errors in the method, but are more than double the net recharge estimated by Gómez-Gómez and Torres-Sierra (1988). This difference could be the result of the discrete nature of net recharge estimates obtained through calibration of a ground-water flow model. Observation wells 11 and 13 are only 700 m north of the cells that Gómez-Gómez and Torres-Sierra (1988) estimated to have net recharge values of 371 mm per year. The net recharge values reported for observation wells 11 and 13 in this report (210 and 230 mm per year) are within the range of values (99 to 371 mm per year) reported by Gómez-Gómez and Torres-Sierra (1988).

The net recharge estimates obtained for observation well 17 are 210 and 220 mm per year for 1995 and 1996, respectively. These net recharge estimates are about 60 percent of the net recharge estimate determined by Gómez-Gómez and Torres-Sierra (1988). This report's estimate of net recharge at well 17 follows the trend of precipitation totals recorded for these years, which were only about 60 to 65 percent of the average reported by NOAA for the area.

The net recharge estimate for observation well 19 in 1988 is higher than the estimates for 1995 and 1996 at observation wells 11, 13, 17, and 19. However, observation well 19 is adjacent to a well developed dry stream bed which probably funnels additional recharge to the aquifer during rainfall events. The net recharge estimates for the Maguayo site (well 19) in 1995 and 1996 are about 80 percent of the value reported by Gómez-Gómez and Torres-Sierra (1988).

The net recharge estimates for the observation well 22 are lower than in other well sites. This probably reflects the higher transmissivity reported by Gómez-Gómez and Torres-Sierra (1988) for this area.

In general the net recharge values for 1995 and 1996 are lower than the average annual values obtained by Gómez-Gómez and Torres-Sierra (1988). The lower net recharge values computed for 1995 and 1996 most probably are related to lower than average annual rainfall.

The net recharge estimates by Gómez-Gómez and Torres-Sierra (1988) are average values for entire cells. It is not surprising that in a heterogeneous karst area, net recharge values at individual well sites would differ from average net recharge values computed for a model grid cell. Considering the differences in the two methods employed, differences in net recharge estimates for these sites by Gómez-Gómez and Torres-Sierra (1988) and from this study are relatively insignificant.

SUMMARY

The upper aquifer near Dorado, Puerto Rico, is a major source of water for both public and private supply. The aquifer is composed of portions of the Aguada Limestone, Aymamón Limestone, and adjacent permeable portions of unconsolidated deposits. As water moves through the aquifer, it changes from a calcium-bicarbonate type in the upgradient portions of the aquifer to a sodium-chloride type in the downgradient portions of the aquifer near the coast. Pumping from the aquifer for industrial use and public supply has lowered the water table to near sea level in some areas, causing saline intrusion to be a concern. The saline-freshwater interface was located by drilling and by borehole geophysics surveys. Drilling and borehole geophysics helped locate the lower limit of the aquifer. The saline-freshwater interface is thin close to the coast and broadens further from the coast. Ground-water hydrographs in the study area were simulated with a deterministic model that allowed calculation of net recharge from precipitation data and ground-water level data. Calculated net recharge rates ranged from 160 mm per year in 1995 at the Santa Rosa well site to 260 mm per year in 1996 at the Maguayo well site. The values obtained for net recharge rates compare favorably with values obtained from ground-water models in the study area.

REFERENCES

Anderson, H.R., 1976, Ground water in the San Juan Metropolitan area, Puerto Rico: U.S. Geological Survey Water-Resources Investigations Report 41–75, 34 p.

Ball, J.W., and Nordstrom, D.K., 1991, User's manual for WATEQ4F, with revised thermodynamic data base and test cases for calculating speciation of major, trace, and redox elements in natural waters: U.S. Geological Survey Open-File Report 91–183, 189 p. (revised and reprinted August 1992).

Berkey, C.P., 1915, Geological reconnaissance of Porto Rico: New York Academy of Science Annals, v. 26, p. 1–70.

_____ 1919, Introduction to the geology of Porto Rico: New York Academy of Science, Scientific Survey of Porto Rico and the Virgin Islands, v. 1, pt. 1, p. 11–29.

Briel, L.I., 1993, Documentation of a multiple-technique computer program for plotting major-ion composition of natural waters: U.S. Geological Survey Open-File Report 93–74, 88 p.

Briggs, R.P., 1966, The blanket sands of northern Puerto Rico, *in* Caribbean Geological Conference, Third, Kingston, Jamaica, 1962, Transactions: Jamaica Geological Survey Publication 95, p. 60–69.

Briggs, R.P., and Akers, J.P., 1965, Hydrogeologic map of Puerto Rico and adjacent islands: U.S. Geological Survey Hydrologic Investigations Atlas HA–197, scale 1:240,000.

Calvesbert, R.J., 1970, Climate of Puerto Rico and U.S. Virgin Islands, revised: U.S. Environmental Science Services Administration, Climatography of the United States 60–52, 29 p.

Day, M.J., 1978, Morphology and distribution of residual limestone hills (mogotes) in the karst of northern Puerto Rico: Geological Society of America Bulletin, v. 89, p. 426–432.

Doerr, A.H., and Hoy, D.R., 1957, Karst landscapes of Cuba, Puerto Rico, and Jamaica: The Scientific Monthly, v. 85, p. 178–187.

Ewers, R.O., Keagy, Dwayne, Quinlan, J.F., and Field, Malcolm, 1989, Discussion of "'Testing' a limestone aquifer using water-table response to storm water discharged into sinkholes" by Andrew Michalski and Joseph Torlucci, Jr.: Ground Water, v. 27, p. 715–716.

Fishman, M.J., and Friedman, M.J., 1989, Methods for determination of inorganic substances in water and fluvial sediments (3d ed.): Techniques of Water-Resources Investigations of the United States Geological Survey, Chapter Al; U.S. Geological Survey Open-File Report, 545 p.

Frost, S.H., Harbour, J.L., Beach, D.K., Realini, M.J., and Harris, P.M., 1983, Oligocene reef tract development southwestern Puerto Rico: Sedimenta IX, University of Miami, Miami Beach, Florida, 144 p.

Giusti, E.V., 1978, Hydrogeology of the karst of Puerto Rico: U.S. Geological Survey Professional Paper 1012, 68 p.

Goddard, E.N., and others, 1948, Rock-color chart: Geological Society of America, 6 p.

Gómez-Gómez, Fernando, 1997, Hurricane Hortense, impact on ground water in Puerto Rico: U.S. Geological Survey Fact Sheet FS–012–97, 2 p.

Gómez-Gómez, Fernando, and Torres-Sierra, Heriberto, 1988, Hydrology and effects of development on the water-table aquifer in the Vega Alta quadrangle, Puerto Rico: U.S. Geological Survey Water-Resources Investigations Report 87–4105, 54 p.

Heisel, J.E., González, J.R., and Cruz, Carlos, 1983, Analog model analysis of the north coast limestone aquifers, Puerto Rico: U.S. Geological Survey Open-File Report 82–52, 49 p.

Hem, J.D., 1985: Study and interpretation of the chemical characteristics of natural water (3d ed.): U.S. Geological Survey Water-Supply Paper 2254, 264 p.

Hubbard, Bela, 1920, The Tertiary formations of Porto Rico: Science, v. 51, p. 395–396.

Hubbard, Bela, 1923, The geology of the Lares District, Porto Rico: New York Academy of Sciences, Scientific Survey of Porto Rico and the Virgin Islands, v. 2, pt. 1, p. 1–115.

Ireland, P., 1979, Geomorphological variation of "case-hardening" in Puerto Rico: Zeitschrift für Geomorphologie, v. 32, p. 9–20.

Kaye, C.A., 1957, The effect of solvent motion on limestone solution: Journal of Geology, v. 65, p. 35–46.

Mack, T.J., 1993, Detection of contaminant plumes by borehole geophysical logging: Ground Water Monitoring and Remediation, v. 12, p. 107–114.

McNeill, J.D., 1986, Geonics EM 39 Borehole Conductivity Meter— Theory of Operation: Mississauga, Ontario, Geonics Limited, Technical Note TN–20, 14 p.

McNeill, J.D., Bosnar, M., and Snelgrove, F.B., 1990, Resolution of an electromagnetic borehole conductivity logger for geotechnical and ground water applications: Mississauga, Ontario, Geonics Limited, Technical Note TN–25, 28 p.

Meyerhoff, H.A., 1938, The texture of karst topography in Cuba and Puerto Rico: Journal of Geomorphology, v. 1, p. 279–295.

_____ 1975, Stratigraphic and petroleum possibilities of middle Tertiary Rocks in Puerto Rico: discussion: American Association of Petroleum Geologists Bulletin, v. 59, p. 169–172.

Michalski, Andrew, and Torlucci, Joseph, Jr., 1988, "Testing" a limestone aquifer using water-table response to storm water discharged into sinkholes: Ground Water, v. 26, p. 751–760.

_____ 1988, Reply to the discussion by R.O. Ewers, Dwayne Keagy, J.F. Quinlan, and Malcolm Field of "'Testing' a limestone aquifer using water-table response to storm water discharged into sinkholes": Ground Water, v. 27, p. 716–717.

Miotke, F.D., 1973, The subsidence of the surface between mogotes in Puerto Rico East of Arecibo (translated from German by W.H. Monroe): Cave and Karst, v. 15, p. 1–12.

Monell-González, Vanessa, 1994, Petrology and geochemistry of groundwater in porous Tertiary carbonate rocks from the North Karst Belt in Dorado, Puerto Rico: Unpublished Masters thesis, Queens College, New York, New York, 110 p.

Monell-González, Vanessa, and González, L.A., 1993, Dolomitization of middle Tertiary carbonates in the north coast Tertiary basin of Puerto Rico (abstract): Geological Society of America, Abstracts with Programs, v. 25, no. 6, p. 161.

Monroe, W.H., 1963, Geology of the Vega Alta quadrangle, Puerto Rico: U.S. Geological Survey Geological Quadrangle Map GQ–191, scale 1:20,000.

_____ 1964, The zanjón, a solution feature of the karst topography in Puerto Rico: U.S. Geological Survey Professional Paper 501–B, p. 126–129.

_____ 1966, Formation of tropical karst topography by limestone solution and reprecipitation: Caribbean Journal of Science, v. 6, p. 1–8.

_____ 1968, The Aguada Limestone of northwestern Puerto Rico: U.S. Geological Survey Bulletin 1274G, 12 p.

_____ 1970, A Glossary of karst terminology: U.S. Geological Survey Water-Supply Paper 1899–K, 26 p.

_____ 1973a, Geological map of the Bayamón quadrangle, Puerto Rico: U.S. Geological Survey Miscellaneous Geologic Investigations Map I–751, scale 1:20,000.

_____ 1973b, Stratigraphic and petroleum possibilities of middle Tertiary Rocks in Puerto Rico: American Association of Petroleum Geologists Bulletin, v. 57, p. 1086–1099.

_____ 1974, Dendritic dry valleys in the cone karst of Puerto Rico: U.S. Geological Survey Journal of Research, v. 2, p. 159–163.

_____ 1975, Stratigraphic and petroleum possibilities of middle Tertiary rocks in Puerto Rico: reply: American Association of Petroleum Geologists Bulletin, v. 59, p. 172–175.

_____ 1976, The karst landforms of Puerto Rico: U.S. Geological Survey Professional Paper 899, 69 p.

_____ 1979, Caves and canyons in the karst belt of northern Puerto Rico: Zeitschrift für Geomorphologie, Neues F. Sup. B.32, p. 21–24.

_____1980a, Geology of the middle Tertiary formations of Puerto Rico: U.S. Geological Survey Professional Paper 953, 93 p.

_____ 1980b, Some tropical landforms of Puerto Rico: U.S. Geological Survey Professional Paper 1159, 39 p.

Monroe, W.H., and Pease, M.H., Jr., 1962, Preliminary geologic map of the Bayamón quadrangle, Puerto Rico: U.S. Geological Survey Miscellaneous Investigations Map I–347, scale 1:20,000.

Moussa, M.T., and Seiglie, G.A., 1975, Stratigraphic and petroleum possibilities of middle Tertiary rocks in Puerto Rico: discussion: American Association of Petroleum Geologists Bulletin, v. 59, p. 163–168.

Moussa, M.T., Seiglie, G.A., Meyerhoff, A.A., and Taner, Irfan, 1987, The Quebradillas Limestone (Miocene-Pliocene), northern Puerto Rico, and tectonics of the northeastern Caribbean margin: Geological Society of America Bulletin, v. 99, p. 427–439.

Nelson, A.E., 1966, Cretaceous and Tertiary rocks in the Corozal quadrangle, northern Puerto Rico: U.S. Geological Survey Bulletin 1244–C, p. 1–20.

Piper, A.M., 1944, A graphic procedure in the geochemical interpretation of water analyses: American Geophysical Union Transactions, v. 25, p. 914–923.

_____ 1953, A graphic procedure in the geochemical interpretation of water analyses [revised]: U.S. Geological Survey Ground Water Notes, Geochemistry, no. 12, 14 p.

Rodríguez-Martínez, Jesús, 1995, Hydrogeology of the north coast limestone aquifer system in Puerto Rico: U.S. Geological Survey Water-Resources Investigations Report 94–4249, 22 p.

Rodríguez-Martínez, Jesús, and Scharlach, R.A., 1994, Geologic and hydrologic data collected at test hole NC–8, Vega Alta, Puerto Rico: U.S. Geological Survey Open-File Report 93–0466, 16 p.

Scharlach, R.A., 1990, Depositional history of Oligocene-Miocene carbonate rocks, subsurface of northeastern, Puerto Rico: New Orleans, Louisiana, University of New Orleans, unpublished Masters Thesis, 174 p.

Seiglie, G.A., and Moussa, M.T., 1984, Late Oligocene-Pliocene transgressive-regressive cycles of sedimentation in northwestern Puerto Rico, *in* Schlee, J.S., editor, Interregional unconformities and hydrocarbon accumulation: American Association of Petroleum Geologists Memoir 36, p. 89–95.

Semmes, D.R., 1919, The geology of the San Juan District, Porto Rico: New York Academy of Sciences, Scientific Survey of Porto Rico and the Virgin Islands, v. 1, pt. 1, p. 33–100.

Sweetings, M.M., 1973, Karst landforms: Columbia Univ. Press, New York, 362 p.

Taylor, K.C., Hess, J.W., and Mazzela, Aldo, 1989, Field evaluation of a slim-hole borehole induction tool: Ground Water Monitoring Review, v. 9, no. 1, p. 100–104.

Thorp, James, 1934, The asymmetry of the "pepino hills" of Puerto Rico in relation to the trade winds: Journal of Geology, v. 42, p. 537–545.

Thrailkill, J.V., 1967, Geology of the Río Camuy Cave area, Puerto Rico, *in* Gurnee, Jeanne, editor, Conservation through commercialization, Río Camuy development proposal: National Speleological Society Bulletin, v. 29, no. 2, p. 35–37.

Torres-González, Arturo, 1983, Hydrologic study of the Río Camuy Cave System, Puerto Rico: unpublished Masters Thesis, University of Puerto Rico, Mayagüez, Puerto Rico, 115 p.

Torres-González, Arturo, and Díaz, J.R., 1984, Water resources of the Sabana Seca to Vega Baja area: U.S. Geological Survey Water-Resources Investigations Report 82–4115, 53 p.

Torres-González, Sigfredo, Planert, Michael, and Rodriguez, J.M., 1996, Hydrogeology and simulation of ground-water flow in the upper aquifer of the Río Camuy to Río Grande de Manatí area, Puerto Rico: U.S. Geological Survey Water-Resources Investigations Report 95–4286, 102 p.

Torres-Sierra, Heriberto, 1985, Potentiometric surface of the upper limestone aquifer in the Dorado-Vega Alta area, north-central Puerto Rico: U.S. Geological Survey Water-Resources Investigations Report 85–4268, scale 1:20,000.

_____ 1997a, Hurricane Hortense, impact on surface water in Puerto Rico: U.S. Geological Survey Fact Sheet FS–014–97, 4 p.

_____ 1997b, Storm-tide elevations caused by Hurricane Marilyn on the U.S. Virgin Islands: U.S. Geological Survey Open-File Report 96–440, 16 plates.

Troester, J.W., 1992, The northern karst belt of Puerto Rico: A humid tropical karst, in Back, William, Herman, J.S., and Paloc, Henri, editors, Hydrogeology of selected karst regions of the world: International Association of Hydrogeologists, International Contributions to Hydrogeology, v. 13, p. 475–486.

_____1994, The geochemistry, hydrogeology, and geomorphology of the Río Camuy drainage basin, Puerto Rico: A humid tropical karst: unpublished Ph.D. dissertation, The Pennsylvania State University, University Park, Pennsylvania, 345 p.

Troester, J.W., White, E.L., and White, W.B., 1984, A comparison of sinkhole depth frequency distributions in temperate and tropical karst regions, *in* Beck, B.F., editor, Sinkholes: their geology, engineering and environmental impact: Proceedings of the First Multidisciplinary Conference on Sinkholes, A.A. Balkema, Rotterdam, p. 65–73.

Troester, J.W., Back, William, and Mora-Castro, S.C., 1987, Karst of the Caribbean, *in* Graf, W.L., editor, Geomorphic Systems of North America: Geologic Society of America, DNAG (Decade of North American Geology) Centennial Special Volume Number 2, p. 347–357.

U.S. Geological Survey, 1998, Water resources data for Puerto Rico and the U.S. Virgin Islands, Water Year 1997: U.S. Geological Survey Water Data Report PR-97-1, 548 p.

U.S. House of Representatives, 1996, Secondary maximum contaminant levels: Code of Federal Regulations, Title 40, Chapter I, Subchapter C, Part 143.

Veve, T.D., and Taggart, B.E., 1996, Atlas of ground-water resources in Puerto Rico and the U.S. Virgin Islands: U.S. Geological Survey Water-Resources Investigations Report 94–4198, 151 p.

Williams, P.W., 1987, Geomorphic inheritance and the development of tower karst: Earth Surface Processes and Landforms, v. 12, p. 453–465.

Williams, J.H., Lapham, W.W., and Barringer, T.H., 1993, Application of electromagnetic logging to contamination investigations in glacial sand-and-gravel aquifers: Ground Water Monitoring and Remediation, v. 12, p. 129–138.

Wood, W.W., 1976, Guidelines for collection and field analysis of ground-water samples for selected unstable constituents: Techniques of Water-Resources Investigations of the United States Geological Survey, Book 1, Chapter D2, 24 p.

Yuan Daoxian, 1985, New observations on tower karst: Proceedings of the First International Conference on Geomorphology, Manchester, England (also published by the Institute of Karst Geology, Guilin, China, 14 p.).

Zapp, A.D., Bergquist, H.R., and Thomas, C.R., 1948, Tertiary geology of the coastal plains of Puerto Rico: U.S. Geological Survey Oil and Gas Investigations Preliminary Map OM–85, 2 sheets, scale 1:60,000.

District Chief
Caribbean District
U.S. Geological Survey
Water Resources Division
GSA Center, Suite 400-15
651 Federal Drive
Guaynabo, Puerto Rico 00965-5703